5101-202
Flat-Plate
Solar Array Project

DOE/JPL-1012-79
Distribution Category UC-63b

(NASA-CR-169919) PHOTOVOLTAIC ARRAY: POWER CONDITIONER INTERFACE CHARACTERISTICS (Jet Propulsion Lab.) 55 p HC A04/MF A01 CSCL 10B

N83-19225

Unclas
G3/44 02873

Photovoltaic Array – Power Conditioner Interface Characteristics

C.C. Gonzalez
G.M. Hill
R.G. Ross, Jr.

December 15, 1982

Prepared for
U.S. Department of Energy
Through an Agreement with
National Aeronautics and Space Administration
by
Jet Propulsion Laboratory
California Institute of Technology
Pasadena, California

(JPL PUBLICATION 82-109)

5101-202
Flat-Plate
Solar Array Project

DOE/JPL-1012-79
Distribution Category UC-63b

Photovoltaic Array – Power Conditioner Interface Characteristics

C.C. Gonzalez
G.M. Hill
R.G. Ross, Jr.

December 15, 1982

Prepared for
U.S. Department of Energy
Through an Agreement with
National Aeronautics and Space Administration
by
Jet Propulsion Laboratory
California Institute of Technology
Pasadena, California

(JPL PUBLICATION 82-109)

Prepared by the Jet Propulsion Laboratory, California Institute of Technology, for the U.S. Department of Energy through an agreement with the National Aeronautics and Space Administration.

The JPL Flat-Plate Solar Array Project is sponsored by the U.S. Department of Energy and is part of the Photovoltaic Energy Systems Program to initiate a major effort toward the development of cost-competitive solar arrays.

This report was prepared as an account of work sponsored by an agency of the United States Government. Neither the United States Government nor any agency thereof, nor any of their employees, makes any warranty, express or implied, or assumes any legal liability or responsibility for the accuracy, completeness, or usefulness of any information, apparatus, product, or process disclosed, or represents that its use would not infringe privately owned rights.

Reference herein to any specific commercial product, process, or service by trade name, trademark, manufacturer, or otherwise, does not necessarily constitute or imply its endorsement, recommendation, or favoring by the United States Government or any agency thereof. The views and opinions of authors expressed herein do not necessarily state or reflect those of the United States Government or any agency thereof.

This publication reports on work done under NASA Task RD-152, Amendment 66, DOE/NASA IAA No. DE-A101-76ET20356.

FOREWORD

The purpose of this report is to provide photovoltaic array and power conditioner subsystem (PCS) designers with the information required to characterize the array-PCS interface.

The Introduction (Section I) presents a general description of array operating characteristics.

The General Analysis Approach section (Section II) provides an overall description of the computer analyses used to characterize the array-PCS interface.

Section III describes the analyses and results obtained when determining the optimum array operating voltage and the gain in available array energy when maximum power tracking is used. In addition, the impact on the results obtained with array degradation is considered.

Section IV addresses the use of protection strategies that can be implemented when any of the array operating parameters (current, power, or voltage) exceeds the upper limits for which the PCS is designed. Also considered is the annual array energy loss for given values of the upper limits and protection strategies used.

Results of the determination of the impact on array energy output of varying the values of array-PCS interface parameters are presented in these Sections III and IV for a number of sites representative of the continental United States.

Section V provides the methodology for estimating the average annual array-PCS efficiency, given the PCS efficiency as a function of PCS output. The annual array energy produced in various power intervals is determined and is a key input in determining the efficiency.

The last section, Section VI, provides a sample problem to guide the reader in the use of the data provided in this report.

ACKNOWLEDGMENT

The authors wish to thank Dahwey Chu and Thomas Key of Sandia National Laboratories and Stan Krauthamer of the Jet Propulsion Laboratory for many useful discussions and suggestions during the performance of the analyses described here.

ABSTRACT

The electrical output (power, current, and voltage) of flat-plate solar arrays changes constantly, due primarily to changes in cell temperature and irradiance level. As a result, array loads such as dc-to-ac power conditioners must be capable of accommodating widely varying input levels while maintaining operation at or near the maximum power point of the array. This report presents the results of an extensive computer simulation study used to define the array operating characteristics and extreme output limits necessary for the systematic design of array-load interfaces under a wide variety of climatic conditions in the U.S.

A number of interface parameters are examined, including optimum operating voltage, voltage tracking width necessary to capture various fractions of the available energy, maximum power and current limits, and maximum open-circuit voltage. The effect of array degradation and I-V curve fill factor on the array-power conditioner interface is also discussed. Results are presented as normalized ratios of power-conditioner parameters to array parameters, making the results universally applicable to a wide variety of system sizes, sites, and operating modes.

PRECEDING PAGE BLANK NOT FILMED

GLOSSARY

Cell temperature	The temperature of a cell at the location of its photovoltaic junction
Center voltage	The central operating voltage about which the voltage is varied in a PCS with maximum power tracking
Concentrator array	A photovoltaic array made up of modules that use concentrated solar radiation and use only the direct normal component of irradiance
Diffuse solar irradiance	The component of incident solar irradiance that results from the atmospheric scatter of the incoming solar radiation
Direct normal solar irradiance	The component of incident solar irradiance which is composed entirely of unscattered solar radiation
E_p	Annual PCS input energy in array power interval P
E_y	Total annual PCS input energy
Efficiency	The ratio of energy output of a device, component, subsystem, or system, to the energy entering it
Extraterrestrial radiation	The solar radiation incident on the earth's atmosphere, before it is scattered by the atmosphere
Fill factor	For any I-V curve, the ratio of maximum power to the product of the open-circuit voltage and short-circuit current
Flat-plate array	A photovoltaic array that uses global solar irradiance without concentration
Fixed-voltage operation	The operation of an array at a constant output voltage
Global solar irradiance	The combined portions of solar irradiance resulting from the scattered and the direct normal component
Ground-mounted array	A photovoltaic array that is mounted in a free-standing configuration and not attached to any building
I_{maxp}	The current produced by a photovoltaic cell, module, or array operating at its maximum power point
I_{sc}	The short-circuit current of a cell, module, or array, which is the current produced with the positive and negative terminals shorted

PRECEDING PAGE BLANK NOT FILMED

Irradiance level (solar)	The amount of power per unit area available from solar radiation
I-V curve	A plot of current versus voltage for a photovoltaic cell, module, or array operating under varying loads ranging from short-circuit to open-circuit
K_1	Fraction of array available annual energy obtained at the PCS input (K_1 = 1 for ideal max power tracking)
K_D	Fraction of total daily extraterrestrial radiation (computed) reaching the earth's surface as diffuse radiation on a horizontal surface
K_T	Total daily radiation on a horizontal surface (measured) at ground level, divided by the total daily extraterrestrial radiation (computed) on a horizontal surface
Maximum open-circuit voltage	The largest expected open-circuit voltage for a given array at a given site
Maximum power point	That point on a cell, module, or array I-V curve where the power is at its maximum value, also known as the maximum power
Maximum power tracking	Continually adjusting the array operating voltage so as to operate always at the array's maximum power point
NOCT	Nominal operating cell temperature; the module (or array) cell temperature when the ambient temperature is 20°C, the incident solar irradiance is 80 mW/cm^2, and wind speed is 1m/sec, with the module (array) open circuited
Normalized to maximum power conditions at SOC	Array power, current or voltage divided by the array maximum power, or current or voltage at maximum power, respectively, under standard operating conditions
Optimum operating voltage	The one fixed array operating voltage that provides the maximum amount of energy from the array over a given period of time
Output power	The power provided at the output terminals of a photovoltaic device, component, subsystem or system
Partial rejection strategy	A strategy for PCS operation, when the array is operating at a power or current level exceeding the maximum allowable limits for the PCS; the operating conditions are changed so that the array operates within allowable limits, resulting in a partial loss (or rejection) of the available array energy at the original operating conditions
PCS	Power conditioner subsystem

Photovoltaic array	An array of photovoltaic modules
P_{SB}	Standby PCS power consumption/h
R	Ratio of PCS full-input-power rating to array maximum power at SOC = Ratio of (PCS full-output-power rating divided by η_1) to array maximum power at SOC
Roof-mounted photovoltaic array	A photovoltaic array that is mounted on the roof of a building either in an integrally attached mode or in a stand-off mode
R_{SB}	P_{SB}/PCS full-output-power rating.
SOC	Standard operating conditions: array operation at a cell temperature of NOCT and irradiance level of 100 mW/cm^2
SOLMET TMY tapes	Data tapes provided by the National Climatic Center containing irradiance and weather data for a Typical Meteorological Year
Total rejection strategy	A strategy for PCS operation: when the array is operating at a power or current level exceeding the maximum allowable limits for the PCS, the array power is totally rejected until the limits are no longer exceeded
τ_{SB}	Hours per year for which PCS has no output power, but draws standby power
V_{maxp}	The voltage across a photovoltaic cell, module, or array operating at its maximum power point
V_{oc}	The open-circuit voltage of a cell, module, or array; the voltage across the positive and negative terminals under open-circuit conditions
Voltage tracking width, window, or range	The range of voltages about a central operating voltage in which a PCS maximum-power tracker operates to obtain the maximum array power in the entire voltage interval
η_1	PCS efficiency at PCS full-power rating
η_P	PCS efficiency for input-power interval P

CONTENTS

I. INTRODUCTION 1

II. GENERAL ANALYSIS APPROACH 5

III. MAXIMIZING ENERGY PRODUCTION. 9

A. FIXED-VOLTAGE OPERATION 9

B. CONTINUOUS-VOLTAGE TRACKING 19

IV. ESTABLISHING MAXIMUM OPERATING LIMITS 25

A. CURRENT AND POWER LIMITS 25

B. VOLTAGE LIMITS 30

V. COMPUTING SYSTEM EFFICIENCY 35

VI. SAMPLE PROBLEM 45

VII. CONCLUSIONS 49

REFERENCES 51

Figures

1. Typical Photovoltaic I-V Curve at 100 mW/cm^2, 25° Cell Temperature 1

2. Influence of Cell Temperature and Irradiance Level on Array I-V Curve 2

3. Typical Shift in I-V Curve to Convert From 25°C to NOCT at 50°C 7

4. Fraction of Annual Array Available Energy Obtained versus Power-Conditioner Fixed Operating Voltage 10

5. Array Optimum Operating Voltage versus Average Daily Maximum Temperature 12

6. Array Annual Energy Loss With Fixed Voltage Operation versus Standard Deviation of Daily Maximum Temperature . . 12

 PRECEDING PAGE BLANK NOT FILMED

7. Array Relative Power Output versus Relative Voltage for Two Fill Factors (0.76 and 0.60) and Two Irradiance Levels 13

8. Optimum Operating Voltage versus Fill Factor 15

9. Percentage of Energy Loss versus Fill Factor 15

10. Rate of Change of Optimum Voltage with Fill Factor versus $\overline{K}_D$ 17

11. Rate of Change of Energy Loss with Fill Factor versus $\overline{K}_D/\overline{K}_T$ 17

12. Annual Array Energy Loss versus Power Degradation 18

13. Percentage Loss in Annual Array Available Energy versus Power-Conditioner Voltage Tracking Range Half Width, Expressed as a Percentage of Optimum Center Voltage 20

14. Effect of Sinusoidal Ripple on Array Energy Output 23

15. Fraction of Annual Array Energy Obtained versus PCS Input-Current Limit for Two Over-Limit Current-Management Strategies 26

16. Fraction of Annual Energy Obtained versus PCS Input-Power Limit for Two Over-Limit Power-Management Strategies 27

17. Maximum Open-Circuit Voltage (from SCLMET TMY) versus Atlas Lowest Recorded Temperature 32

18. Illustration of the Construction Principle Behind a Plot of Normalized Power versus Operating Time With the Time Intervals Ordered According to Decreasing Power Level 35

19. Hours of Array Operation versus Array Power Level During One Year 36

20. Typical Power-Conditioner Efficiency vs Fraction of Power-Conditioner Full-Output Power Rating and Array Maximum Power at SOC 39

21. Effect of Typical Power-Conditioner Efficiency on Array Annual Power Production 42

22. Composite of Annual Array Power Level versus Operating Hours for 26 Sites 42

Tables

1. Typical Cell Parameters 8

2. Simulation Results for Fixed-Voltage Power Conditioner. . . 11

3. Effect of Fill Factor on Fixed-Voltage Operation Results. . 14

4. Shift in Array Fill Factor With Array Power Degradation . . 19

5. Shift in Optimum Operating Voltage With Array Power Degradation 19

6. Simulation Results for Continuous-Tracking Power Conditioner 21

7. Sensitivity of Continuous-Tracking Parameters to Array Fill Factor 22

8. Effect of Partial and Total Rejection Strategies on Power and Current Limits versus Fraction of Available Energy Obtained 28

9. Effect of Array Fill Factor on Power and Current Limits Required to Obtain Various Fractions of Available Energy 29

10. Estimated Maximum Open-Circuit Voltage for 26 Sites 31

11. Fraction of Annual Array Energy Available in Various Relative Power Intervals for 26 Sites 37

12. Example Average Annual Efficiency Calculation for Albuquerque 41

13. Operating and Maximum Parameters. 46

14. Average Annual Efficiency Calculation for Composite of All 26 Sites 47

ORIGINAL PAGE IS
OF POOR QUALITY

SECTION I

INTRODUCTION

The electrical output over time of photovoltaic (PV) arrays is unusual in comparison with that of conventional electrical power generators, and requires careful consideration if efficient and reliable system performance is to be achieved.

Many electrical generators can be characterized as either constant-voltage or constant-current sources; PV arrays exhibit the characteristics of both, depending on the operating point (load impedance). In addition, the output voltage and current of the array are directly controlled by the array temperature and irradiance level, respectively.

Figure 1 illustrates the typical current-voltage (I-V) characteristic of an array at a particular irradiance level (100 mW/cm^2) and cell temperature (25°C). These conditions, referred to as peak reporting conditions, have been adopted as a standard for reporting peak array output by the international photovoltaic community (Reference 1). As Figure 1 shows, the array performs more or less as a constant-current source when feeding lower

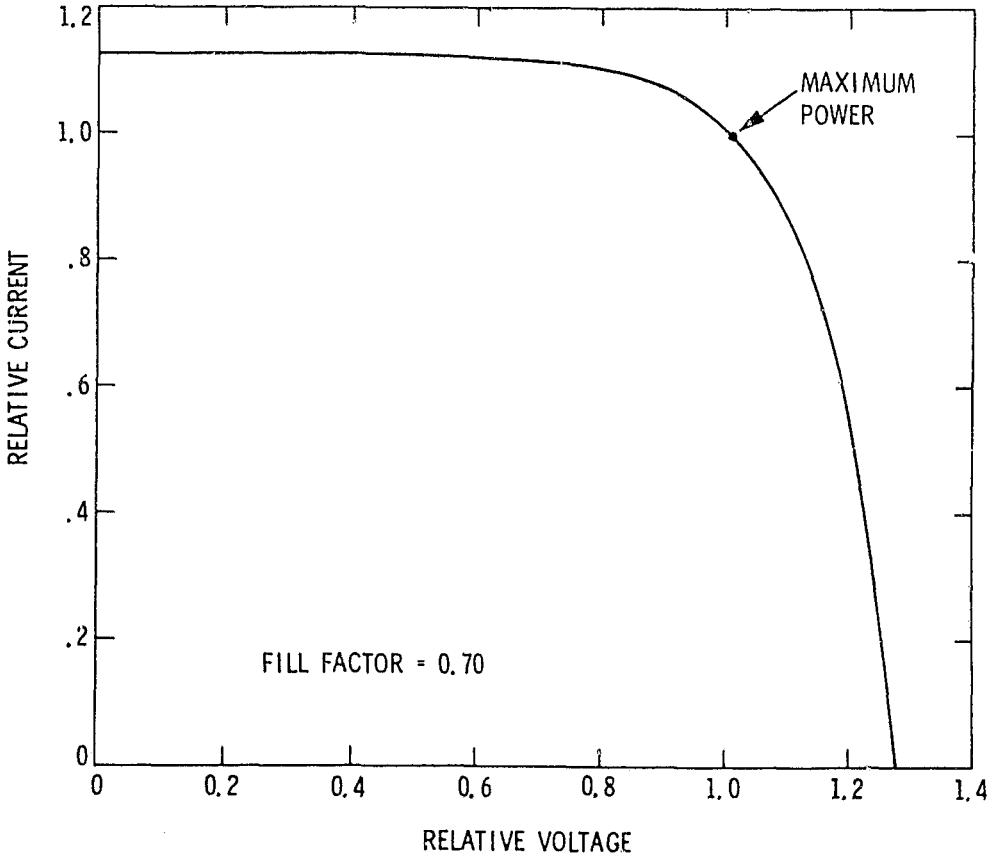

Figure 1. Typical Photovoltaic I-V Curve at 100 mW/cm^2, 25°C Cell Temperature

ORIGINAL PAGE IS
OF POOR QUALITY

impedance loads and as a constant-voltage source when feeding higher impedance loads. The maximum power output is generated at a point on the knee of the curve referred to as the maximum power point.

Figure 2 shows how the I-V characteristic varies with changing cell temperature and irradiance level. In general, the short-circuit current of the array is directly proportional to the irradiance level, and the voltage at the maximum power point is linearly dependent upon cell temperature, decreasing about 0.5% of its 25°C value for each 1°C of increasing cell temperature.

Because of this strong dependence on irradiance level and cell temperature, the output of a photovoltaic array is highly dependent on weather conditions and array construction practices that influence these parameters. If maximum energy is to be drawn from the array, the load interfacing with the array must be designed to accommodate these site-specific and time-dependent changes in array output. In addition, maximum current, voltage and power ratings of the load must be compatible with the maximum levels that the array can deliver.

In most residential applications, the load on the photovoltaic array will be a power-conditioning subsystem (PCS) designed to convert the direct current (dc) array output into alternating current (ac), the form supplied by utilities to typical residential users. In this case the PCS is responsible for accommodating the widely varying array output and maximizing energy production.

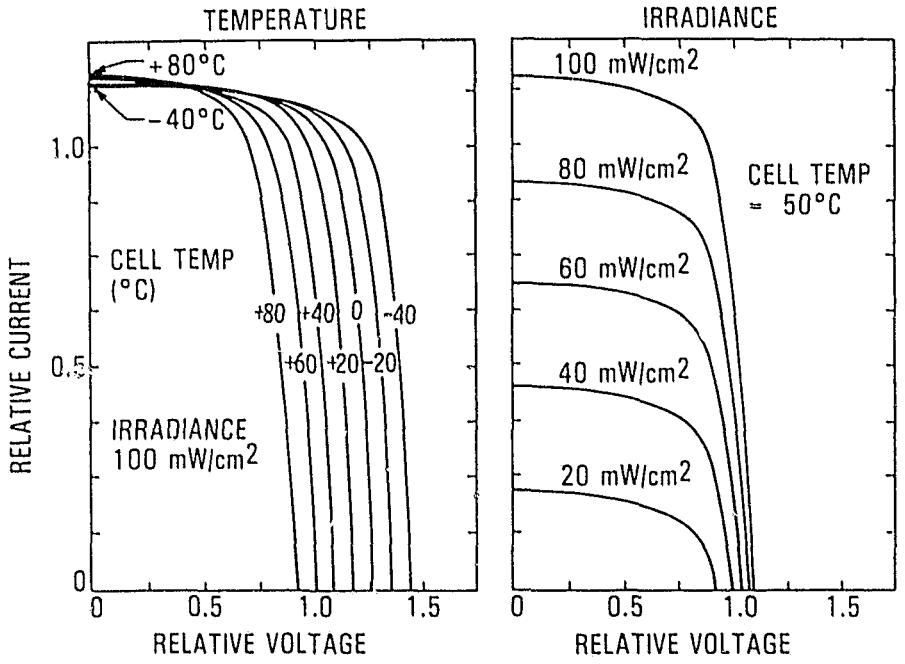

Figure 2. Influence of Cell Temperature and Irradiance Level on Array I-V Curve

In other systems, with direct-current loads, the dc-to-dc converter or storage battery and charging system must provide these functions. Regardless of the type of operating system, the long-term array output characteristics for the application site of interest are necessary ingredients in efficient system design.

To aid the designer in understanding these effects, and for making proper system tradeoffs, this document summarizes an extensive study conducted by the Jet Propulsion Laboratory (JPL) to characterize the output of flat-plate arrays for a variety of operating conditions typical of sites throughout the United States. The limitation to flat-plate arrays stems from the use of weather data for total irradiance on fixed-tilt flat surfaces, as opposed to the direct-normal irradiance that would be used for tracking concentrator arrays.

After the following section, which provides an overview of the general analysis approach, each remaining section treats one aspect of array performance and its influence on the design of array loading systems. These include:

(1) Maximum Power Tracking

  (a) Fixed-voltage operation versus voltage tracking.

  (b) Voltage-tracking-width tradeoffs with continuous-voltage tracking.

(2) Array Extreme-Value Analysis

  (a) Short-circuit current.

  (b) Maximum power.

  (c) Open-circuit voltage.

(3) PCS/Converter Efficiency Calculation

  (a) Array energy output versus power level.

  (b) Operating hours at various relative power levels.

To clarify the concepts presented, extensive use is made of design examples.

SECTION II

GENERAL ANALYSIS APPROACH

Definition of the relationships between typical array performance and various kinds of loading required the simulation of typical array performance for a variety of representative long-term operating conditions. This simulation was accomplished using a computer to calculate hourly electrical output for a period of a year at each of 26 sites in the United States. Hourly weather data were obtained using solar radiation surface meteorological observations (SOLMET) typical meteorological year (TMY) weather data tapes containing historical measurements for a typical meteorological year at each site.

The hourly irradiance level on the array was derived from the SOLMET irradiance data using an algorithm developed by Klucher and based on the work of Liu-Jordan (see Reference 1 for a detailed description of the algorithms). The array was assumed to be a flat, south-facing surface tilted up from the horizontal at an angle equal to the latitude of the site. The hourly photovoltaic cell temperature was then computed based on the irradiance level incident on the array, and the hourly ambient air temperature from the SOLMET data tape. The cell temperature is computed with an algorithm developed at JPL based on experimental data.

The equation used is given by:

$$T_{cell} = T_{amb} + KS$$

where:

T_{cell} is the computed photovoltaic cell temperature

T_{amb} is the ambient temperature value (from SOLMET tape)

K is an empirically determined constant

S is the solar irradiance.

The constant K includes the effect of a constant low-level wind environment. It has been determined at JPL (Reference 2) that the temperature of an array in the midst of an array field is relatively insensitive to wind speed, which is kept low by the presence of the field. The wind speed, typically recorded on SOLMET tapes, is much higher than the wind speed found at ground level and is not directly usable.

Hourly electrical performance was derived using a baseline I-V curve selected as representative of a present-day silicon-cell array (Figure 1). The array I-V curve is defined initially at 25°C and an irradiance level of 100 mW/cm^2 and is then translated to the hourly cell-temperature, irradiance-level conditions to determine the hourly values of the power and operating parameters.

PAGE 4 INTENTIONALLY BLANK

PRECEDING PAGE BLANK NOT FILMED

Because the shape of I-V curves varies somewhat for different manufacturers and for different degrees of degradation with age, other I-V curves were also used to define the sensitivity of the simulation results to curve shape. The shape, or squareness, of I-V curves is generally quantified by the fill factor, which is defined as the ratio of maximum power to the product of open-circuit voltage and short-circuit current as given by the following:

$$\text{Fill factor (at } 25^{\circ}\text{C)} = \frac{\text{Max Power (at } 25^{\circ}\text{C)}}{I_{sc} \times V_{oc} \text{ (at } 25^{\circ}\text{C)}}$$

With this definition a perfectly rectangular I-V curve would have a fill factor of 1.0, and a straight I-V curve would have a fill factor of 0.25. Typical curves for new arrays have fill factors averaging around 0.70, and ranging from 0.60 to 0.76. As an array ages its fill factor often decreases, reflecting degradation associated with increased series resistance. Fill factors ranging from 0.45 to 0.75 (at 25°C, 100 mW/cm^2) were used in the sensitivity results presented here.

Once the array I-V curves were obtained for each hourly irradiance level and cell temperature, the annual energy production was calculated using a variety of array loading strategies. The extreme array output levels were obtained by scanning the hourly I-V curves. The results of these analyses are presented in the remainder of this report.

To make the results as generally applicable as possible, the data are presented as ratios of normalized load characteristics to normalized array characteristics at standard operating conditions (100 mW/cm^2, NOCT).

Standard operating conditions are a second set of recognized reference conditions for rating photovoltaic arrays and are different from peak rating conditions (100 mW/cm^2, 25°C) in that they use NOCT for the chosen PV modules in the intended mounting configuration, instead of the fixed 25°C cell temperature selected for convenience in laboratory measurements. Use of NOCT makes the results of this study generally independent of operating temperature differences associated with modules and arrays with different thermal heat-transfer properties.

Site-to-site weather-related operating temperature differences are included separately through the presentation of site-specific results.

The NOCT for an array is defined as the operating temperature of the cells in the intended mounting configuration with incident irradiance level of 80 mW/cm^2, air temperature of 20°C, wind velocity of 1 m/s, and the array open-circuited. This set of conditions yields a temperature that accurately represents the average cell temperature in the field during periods of significant energy production (Reference 1). Roughly 50% of the energy will be produced above and 50% below this temperature. Typical values of NOCT for ground-mounted arrays range from 45° to 50°C, and for roof-mounted arrays from 60° to 70°C.

ORIGINAL PAGE IS
OF POOR QUALITY

The I-V curve at SOC for an array of interest can be approximated closely from the I-V curve at peak rating conditions by subtracting a voltage offset (shifting the curve to the left, parallel to the voltage axis) by an amount equal to 0.5% of the maximum power voltage at 25°C multiplied by the temperature difference (NOCT -25°C) (Figure 3).

Table 1 presents some average values of cell parameters measured at JPL for typical single-crystal silicon solar-cell modules. The values in the table provide an indication of what actual NOCT values to expect for current modules. The rate of I-V curve voltage translation with temperature in the vicinity of the maximum power point is given for several modules; this led to the selection of 0.5% for this study (i.e., $5 \times 10^{-3} \times V_{maxp}$ (at 25°C, 100 mW/cm^2) per °C). The rate of current translation with temperature in the vicinity of the maximum power point is .04% (i.e., 4×10^{-4} I_{maxp} (at 25°C, 100 mW/cm^2) per °C). The rates of change of current and voltage discussed here are strictly valid only in the region of the maximum power point and should not be used to determine open-circuit voltage or short-circuit current changes.

Most of the results that follow are presented in terms of the current, voltage or power produced by the array at its maximum power point under SOC conditions. For the sake of brevity, these values are referred to as the maximum power current at SOC, the maximum power voltage at SOC and the maximum power at SOC.

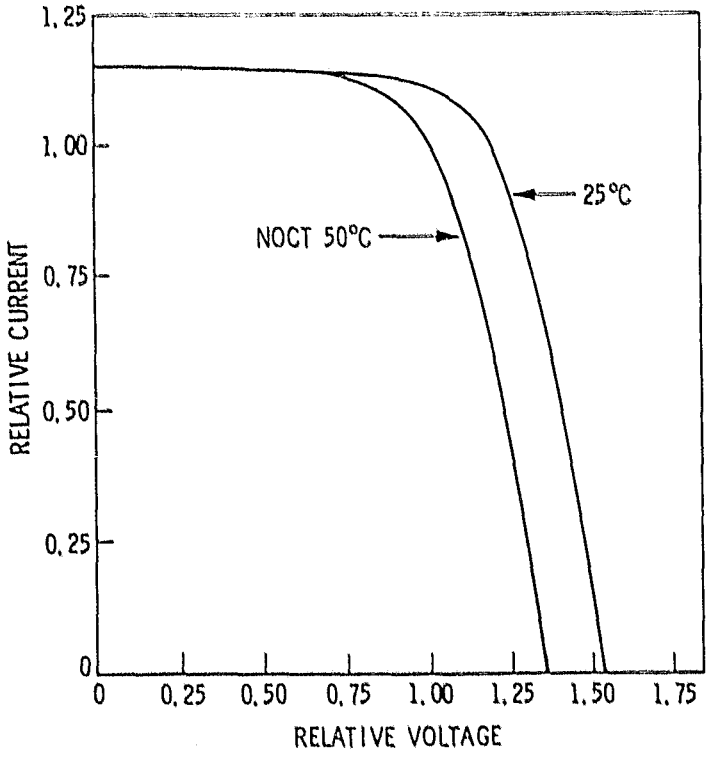

Figure 3. Typical Shift in I-V Curve to Convert From 25°C to NOCT at 50°C

ORIGINAL PAGE IS
OF POOR QUALITY

Table 1. Typical Parameters for Crystalline Silicon Solar Cells in Terrestrial Modules

Module Type	NOCT, °C	$\Delta V/\Delta T$*, % of V_{maxp} at 25° per °C	Solar Cell V_{maxp} at 25°C, V	Solar Cell V_{maxp} at NOCT, V
A	43.2	0.47	0.463	0.426
B	41.1	0.50	0.460	0.433
C	52.8	0.45	0.500	0.447
D	46.0	0.44	0.475	0.430
E	49.8	0.54	0.458	0.401
F	48.6	0.48	0.495	0.437
G	45.6	0.53	0.481	0.432
H	56.0**	0.53	0.468	0.403
I	48.8**	0.56	0.438	0.392
Average of All Modules	48.0	0.50	0.471	0.422

*$\Delta I/\Delta T$, .04% of I_{maxp} at 25°C (100 mW/cm^2) per °C.

**Residential module

SECTION III

MAXIMIZING ENERGY PRODUCTION

To achieve maximum energy output from the array under field operating conditions requires that the power conditioner maintain operation at (or track) the maximum power point. A variety of candidate strategies are available:

(1) Operation at constant voltage, assuming that the primary changes in array output are current variations associated with changing illumination level.

(2) Seasonally or infrequently adjusted constant voltage operation to account for seasonal temperature trends and/or array degradation.

(3) Constant voltage operation with voltage updating based on frequent temperature sensing.

(4) Continuous closed-loop feedback sensing of the PCS output power to achieve continuous operation at the maximum power point (some systems of this type actually result in local oscillation about the maximum power point as a result of the control algorithm).

A key consideration in the tradeoff between fixed-voltage operation or some form of periodic or continuous voltage tracking is the gain in array energy that can be achieved. A second consideration is selection of the optimum fixed voltage or voltage window limits with respect to the array voltage rating.

To provide a data base for these decisions the relative annual energy performance was determined for a large number of fixed-voltage systems with different fixed voltages and for an ideal continuous-tracking system. Sensitivity studies were then conducted using other array fill factors.

A. FIXED-VOLTAGE OPERATION

Figure 4 presents an example plot of normalized energy output versus normalized power-conditioner voltage for Albuquerque, New Mexico. The ordinate scale in this plot is the fraction of available energy drawn from the array during the indicated period of the year (spring and fall, summer, winter and full year) by a constant-voltage system. The ratio of the PCS operating voltage to the array maximum-power voltage (V_{maxp}) at SOC is indicated on the abscissa. This plot for Albuquerque indicates, for example, that the optimum voltage without seasonal adjustment is approximately 96% of the array V_{maxp} at SOC, and that this fixed voltage system will lose about 2% of the available energy. If seasonal adjustment is used, the voltage should vary from about 92% of V_{maxp} in the summer to 103% of V_{maxp} in the winter and the energy loss will be reduced to about 1%.

ORIGINAL PAGE IS
OF POOR QUALITY

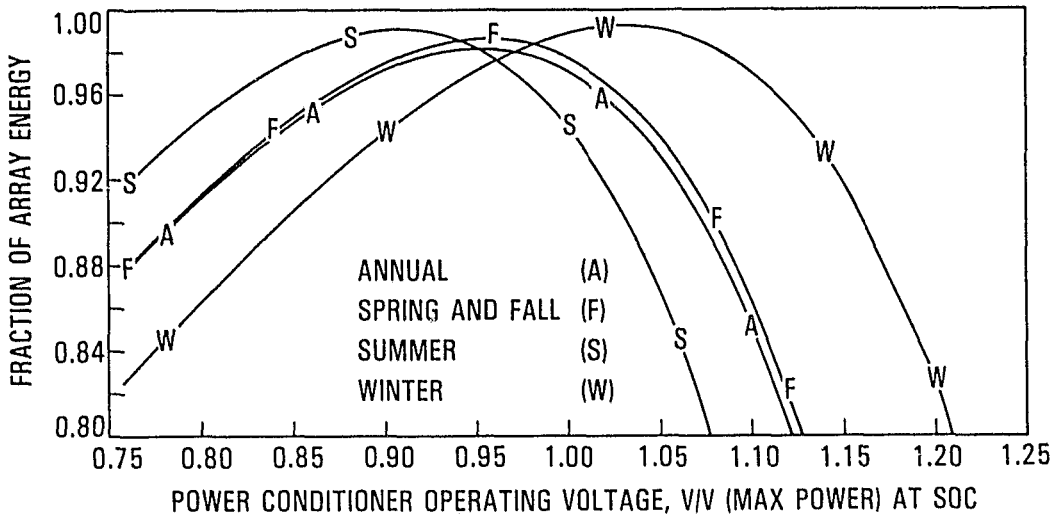

Figure 4. Fraction of Annual Array Available Energy Obtained versus Power-Conditioner Fixed Operating Voltage (Albuquerque NM)

Table 2 summarizes the key findings for the 26 sites. The following data are provided:

(1) The optimum fixed voltage with and without seasonal adjustment for each site.

(2) The percentage loss in available annual energy with the optimum fixed voltage.

(3) The percentage loss in available annual energy with the use of seasonally adjusted fixed voltage operation.

The tabular data show that the optimum fixed voltage ranges from about 92% of the array voltage for hot climates such as Phoenix to 100% of the array voltage for colder climates such as Caribou, Maine. In addition, the data show that the fraction of annual available energy that is lost by a fixed-voltage system ranges from 0.7% to 2.5%, with few sites over 2%. Seasonal adjustment of the power-conditioner operating voltage reduces the fixed-voltage losses by 15% to 30%.

To extend the appliability of the results presented to sites other than the 26 sites analyzed, a regression analysis was performed to examine possible correlations between historical site daily maximum temperatures and the observed optimum operating voltage and annual energy loss. Figures 5 and 6 show the results obtained when the simulation results for the 26 SOLMET sites investigated were correlated with the maximum temperature data from a standard atlas (Reference 4). The optimum operating voltage correlates well with the annual average maximum temperature and the percentage of energy lost with the standard deviation of the monthly averages of daily maximum temperature. The curves provide a ready means of estimating optimum voltage and annual energy loss with the use of monthly average daily maximum temperatures obtained from any weather atlas or from long-term recorded weather data.

Table 2. Simulation Results for Fixed-Voltage Power Conditioner

Site	Fixed-Voltage Power-Conditioner Optimum Operating Voltage (V_{op}/V_{maxp} at SOC)				% Loss in Energy with Fixed Voltage Power Conditioner (no seasonal adjustment)	% Loss in Energy with Fixed Voltage Power Conditioner (with seasonal adjustment)
	Annual	Spring & Fall	Summer	Winter		
Albuquerque NM	0.96	0.96	0.92	1.03	1.7	1.0
Apalachicola FL	0.94	0.94	0.91	0.97	1.1	0.9
Bismarck ND	0.97	0.98	0.94	1.07	2.5	1.9
Boston MA	0.97	0.98	0.94	1.03	2.0	1.7
Brownsville TX	0.92	0.92	0.91	0.95	0.8	0.7
Cape Hatteras NC	0.95	0.96	0.93	0.99	1.3	1.1
Caribou ME	1.00	1.01	0.96	1.06	2.2	1.8
Charleston SC	0.95	0.95	0.93	0.98	1.1	0.9
Columbia MO	0.96	0.96	0.92	1.02	2.0	1.5
Dodge City KS	0.95	0.96	0.92	1.03	1.9	1.4
El Paso TX	0.94	0.94	0.91	1.00	1.3	0.9
Ely NV	0.98	0.98	0.95	1.05	1.7	1.2
Fort Worth TX	0.93	0.94	0.91	0.98	1.5	1.2
Fresno CA	0.94	0.94	0.91	1.00	1.3	1.0
Great Falls MT	0.97	0.98	0.94	1.04	2.0	1.6
Lake Charles LA	0.93	0.93	0.92	0.97	1.1	1.0
Madison MI	0.97	0.98	0.94	1.05	2.3	1.8
Medford OR	0.96	0.96	0.94	1.00	1.4	1.3
Miami FL	0.93	0.93	0.92	0.94	0.7	0.6
Nashville TN	0.95	0.95	0.93	1.00	1.6	1.4
New York NY	0.97	0.98	0.95	1.02	1.7	1.5
Omaha NB	0.96	0.97	0.93	1.04	2.1	1.6
Phoenix AZ	0.92	0.92	0.89	0.97	1.4	1.0
Santa Maria CA	0.97	0.97	0.96	0.98	0.7	0.7
Seattle WA	0.97	0.97	0.96	0.97	1.4	1.3
Sterling VA (Washington DC)	0.96	0.96	0.94	1.02	1.7	1.3

ORIGINAL PAGE IS OF POOR QUALITY

ORIGINAL PAGE IS
OF POOR QUALITY

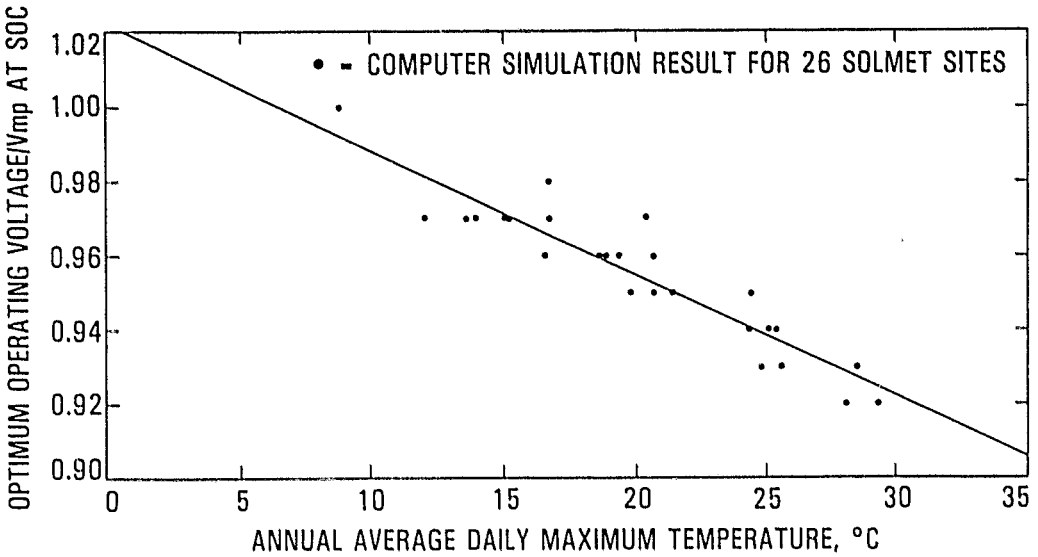

Figure 5. Array Optimum Operating Voltage versus Average Daily Maximum Temperature

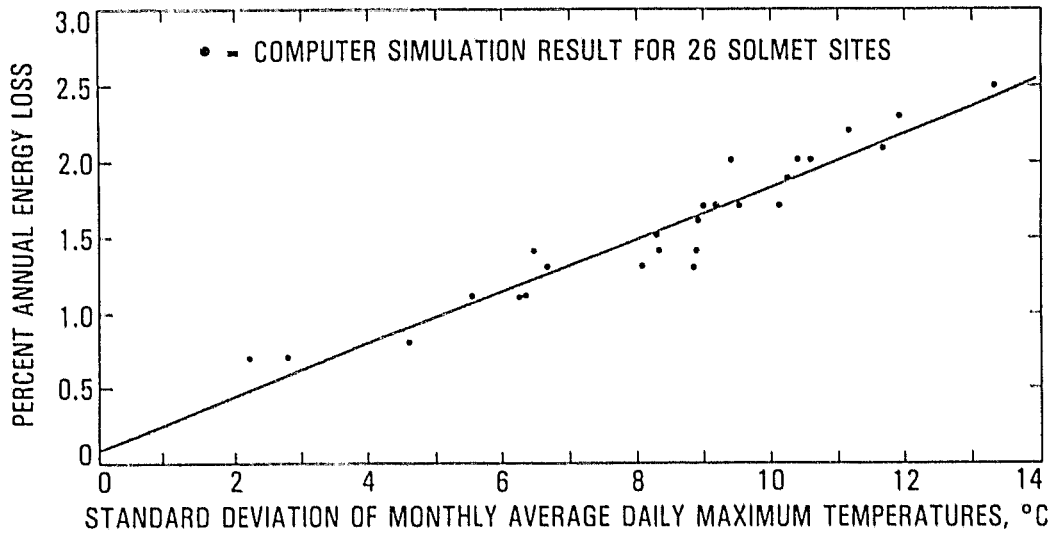

Figure 6. Array Annual Energy Loss With Fixed-Voltage Operation versus Standard Deviation of Daily Maximum Temperature

ORIGINAL PAGE IS
OF POOR QUALITY

1. Effect of I-V Curve Fill Factor on Optimum Operating Voltage

Another parameter that has a modest effect on selection of the optimum operating voltage is the array fill factor. Figure 7 illustrates the key differences between a high (0.76) and low (0.60) fill factor. As noted, high fill factors lead to sharper voltage peaks and little maximum-power-voltage variation with irradiance level. In contrast, low fill factors lead to flatter optimums, but to larger variations in maximum power voltage with irradiance level. Therefore, the tendency is for high-fill-factor arrays to be more sensitive to large environmental temperature swings because of their sharp power-voltage peaks, and for low-fill-factor arrays to be more sensitive to low irradiance levels (cloudy sites) because of their voltage shifts with irradiance. The data in Table 2 are for a nominal fill factor of 0.7.

Table 3 describes the sensitivity of the fixed-voltage-operation results to array I-V curve fill factor for five representative sites. The results indicate a modest trend toward increasing power-conditioner voltages with higher fill factors, and small changes in annual energy losses.

Figures 8 and 9 display graphically the site dependence of the fill-factor influence on optimum operating voltage and annual energy loss for two of the sites, Boston and Albuquerque.

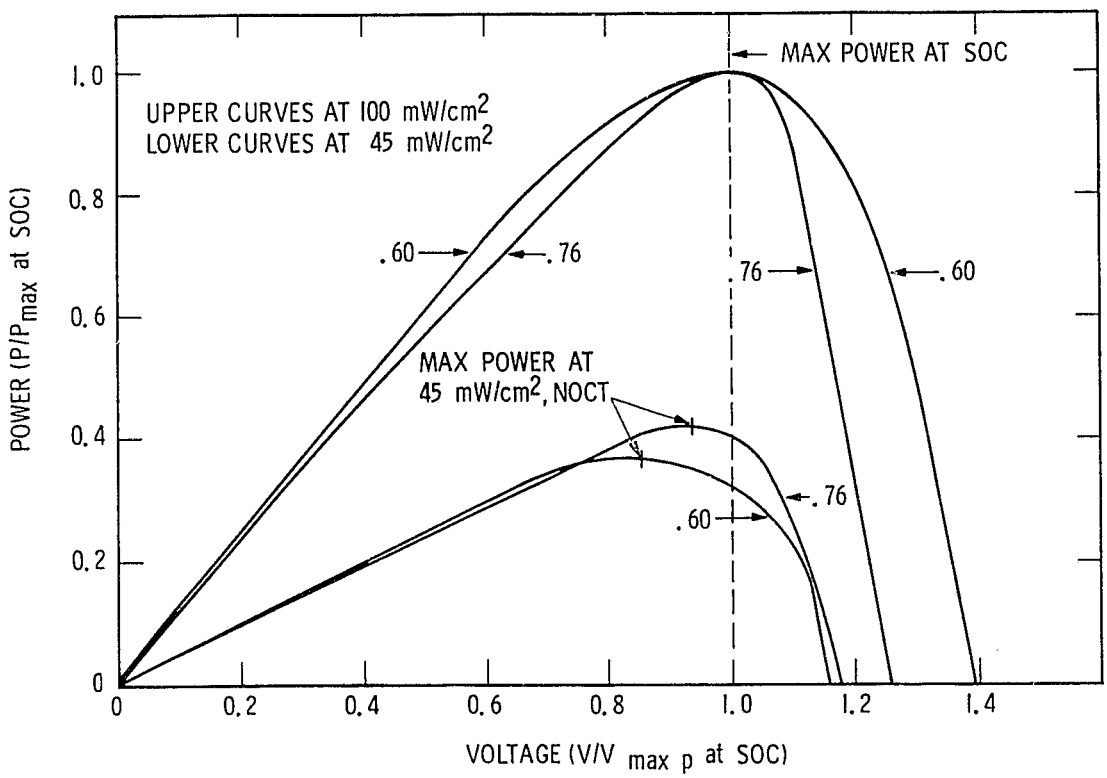

Figure 7. Array Relative Power Output versus Relative Voltage for Two Fill Factors (0.76 and 0.60) and Two Irradiance Levels

ORIGINAL PAGE IS
OF POOR QUALITY

Table 3. Effect of Fill Factor on Fixed-Voltage Operation Results

Site	Fill Factor	Optimum Operating Voltage	% Loss in Energy With Fixed-Voltage Power Conditioner
Albuquerque	0.45	0.90	2.4
	0.50	0.91	2.0
	0.55	0.93	1.8
	0.60	0.94	1.8
	0.65	0.95	1.7
	0.70	0.96	1.7
	0.75	0.96	2.2
Bismarck	0.45	0.88	3.5
	0.50	0.90	3.2
	0.55	0.93	3.0
	0.60	0.95	2.9
	0.65	0.96	2.8
	0.70	0.97	2.5
	0.75	0.99	3.0
Boston	0.45	0.85	3.5
	0.50	0.88	3.4
	0.55	0.90	3.3
	0.60	0.92	3.2
	0.65	0.94	2.8
	0.70	0.97	2.0
	0.75	0.99	1.9
Miami	0.45	0.80	1.8
	0.50	0.83	1.6
	0.55	0.86	1.3
	0.60	0.88	1.2
	0.65	0.90	1.0
	0.70	0.93	0.7
	0.75	0.95	0.6
Phoenix	0.45	0.85	1.9
	0.50	0.87	1.7
	0.55	0.89	1.6
	0.60	0.90	1.5
	0.65	0.91	1.4
	0.70	0.92	1.4
	0.75	0.92	1.8

ORIGINAL PAGE IS
OF POOR QUALITY

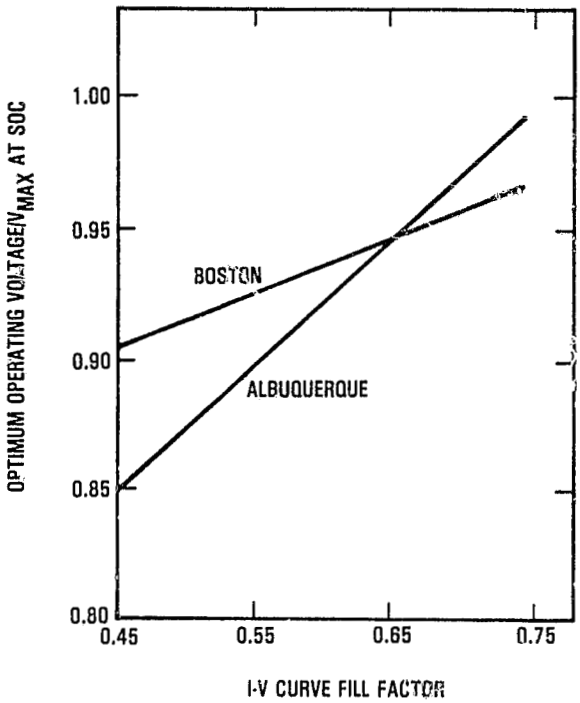

Figure 8. Optimum Operating Voltage versus Fill Factor

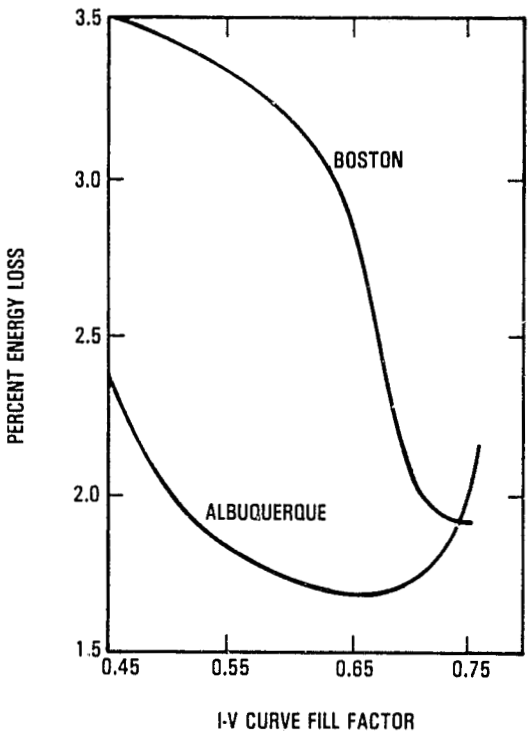

Figure 9. Percentage of Energy Loss versus Fill Factor

To allow extension of the limited results shown to additional sites, an analysis was performed attempting to correlate the observed site dependencies of fill factor to commonly available weather parameters. It was observed from Table 3 that in general the magnitude of the rate of change in optimum operating voltage and energy loss increases for those sites characterized by a significant amount of cloudiness; conversely, low values of rate of change are associated with sites known for having a high percentage of sunny days. With this observation, the fractional change in optimum voltage with fill factor was compared with the fraction of total daily extraterrestrial radiation reaching the Earth's surface as diffuse (scattered) radiation on a horizontal surface. This parameter is commonly available in solar energy atlases such as Reference 4 and is referred to as the K_D index for the site. It is computed for each day of the month and is condensed into an average that represents a typical day for the month. A companion index is the K_T index, defined as the total daily radiation on a horizontal surface at ground level divided by the total daily extraterrestrial radiation on a horizontal surface (i.e., the index is also computed for each day in the month and is condensed into an average that represents a typical day for the month). The percentage of energy lost in fixed-voltage operation as a function of fill factor was correlated with the ratio of the annual average of the K_D ($\overline{K}_D$) and K_T ($\overline{K}_T$) indices obtained by averaging monthly values given in Reference 4.

The two correlations discussed above are shown in Figures 10 and 11 for 11 sites. The sites analyzed can be divided into cloudy sites (higher values of K_D) and clear sites (lower values of K_D). The two relationships shown in Figures 10 and 11 can be used to estimate the expected spread in optimum voltage and percentage of energy lost for sites in the United States.

Reference 4 has an extensive table of monthly K_D and K_T values. The variation in these values from site to site is limited; thus estimates for a given site could be made from the values at adjacent sites.

In summary, the recommended procedure for systems designers is to use the correlations given by Figures 5 and 6 and the atlas values for maximum temperature to obtain optimum operating voltage and percentage of energy loss for an I-V curve with a fill factor of 0.7. This should be followed by use of a reference such as Reference 4 to obtain annual average values of the K_D and K_T indices and use of the correlation given in Figures 10 and 11 to obtain an estimate of the variations of optimum voltage and percentage of energy loss with fill factor. In addition to the correlations developed, Tables 2 and 3, which provide data for a limited number of sites, can be used to provide estimates of desired parameters at other sites having similar climatic characteristics.

2. Effect of Array Degradation on Optimum Operating Voltage

Another factor affecting the selection of a fixed-voltage operating system is the expected change in the optimum operating voltage as an array degrades. This change has two components: one is associated with the dropping of the maximum power voltage at SOC as the array degrades; the second is associated with the change in the ratio of the optimum voltage to the V_{maxp} at SOC because array degradation generally is manifested as a change in array fill factor. The effect of fill-factor change alone is described in the previous section.

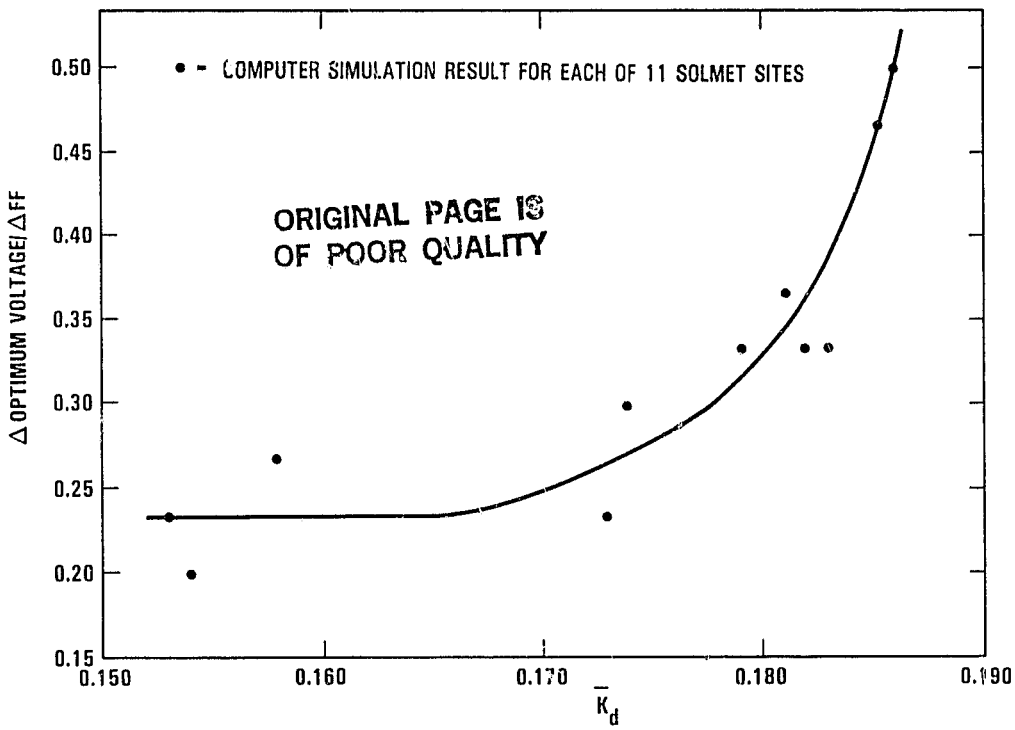

Figure 10. Rate of Change of Optimum Voltage with Fill Factor versus $\bar{K}_D$

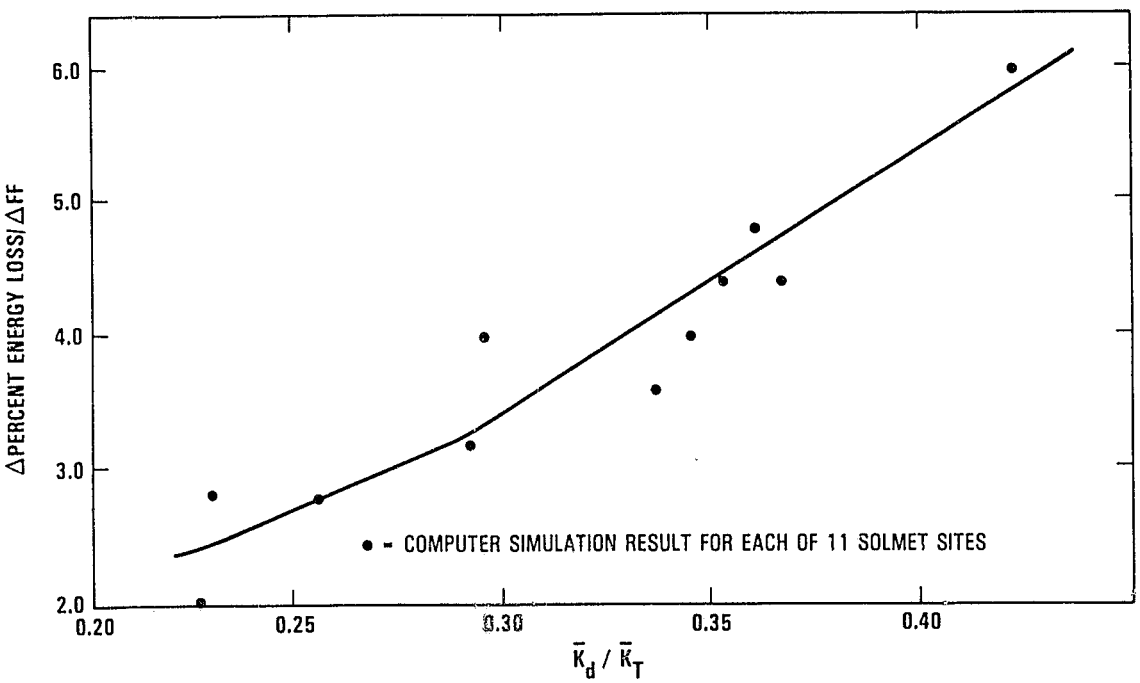

Figure 11. Rate of Change of Energy Loss with Fill Factor versus $\bar{K}_D/\bar{K}_T$

ORIGINAL PAGE IS
OF POOR QUALITY

Because array degradation should only be significant over long periods of time, one means of dealing with array degradation is to provide for periodic updating of the optimum voltage setting of the PCS throughout the system life. If the voltage is not updated, the annual energy losses will increase as the fixed voltage becomes too high for the degraded array. Figure 12 illustrates the annual array energy loss as a function of the percentage o power degradation for an array continuously operated at the initial optimum fixed voltage throughout the time it was degrading. Also shown in Figure 12 for comparison are the annual array energy loss if continuous maximum power tracking is provided and the annual energy loss (dotted line) for updated fixed voltage operation where the operating voltage is continually adjusted to match the array degradation.

An important observation from Figure 12 is that the annual energy output of an array degrades about 1.4 times as fast as its power rating at SOC, even with an ideal maximum power tracker. This has significant economic implications relative to the worth of heavily degraded systems or, more correctly, to the worth of arrays with poor fill factors.

Tables 4 and 5 provide estimates of the fill-factor decrease likely to be associated with a given level of power degradation, and the total shift in optimum operating voltage required to accommodate the altered operating characteristics. Data are provided for three initial (new array) fill factors of 0.75, 0.70 and 0.65.

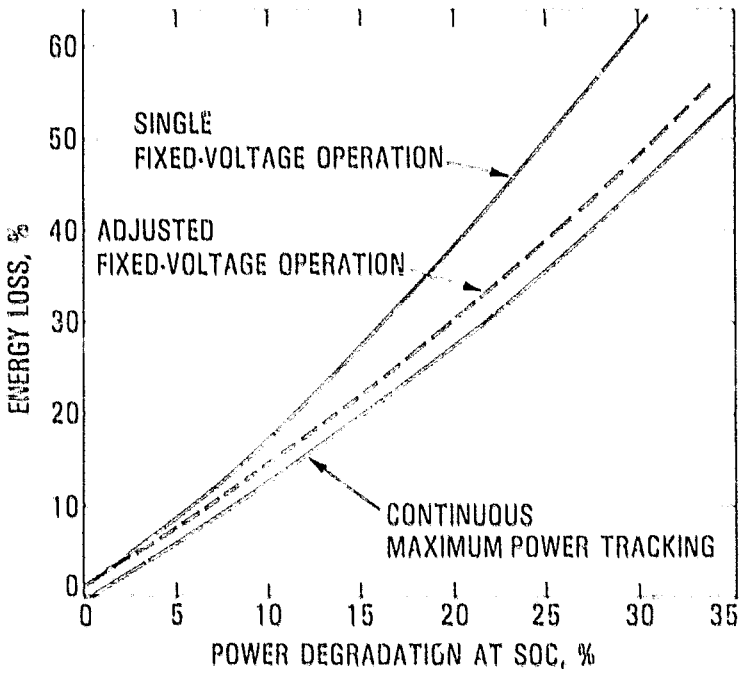

Figure 12. Annual Array Energy Loss versus Power Degradation

Table 4. Drop in Array Fill Factor With Array Power Degradation

Maximum Power Initial Maximum Power	Initial Fill Factor:	Fill Factor (0.75)	(0.70)	(0.65)
1.00		0.75	0.70	0.65
0.95		0.73	0.67	0.61
0.90		0.70	0.63	0.57
0.85		0.67	0.59	0.53
0.80		0.63	0.54	0.48
0.75		0.59	0.49	0.43
0.70		0.53	0.43	0.37

Table 5. Shift in Optimum Operating Voltage With Array Power Degradation

Maximum Power Initial Maximum Power	Initial Fill Factor:	Optimum Operating Voltage Initial Optimum Operating Voltage (0.75)	(0.70)	(0.65)
1.00		1.000	1.000	1.000
0.95		0.975	0.975	0.975
0.90		0.950	0.950	0.950
0.85		0.925	0.925	0.930
0.80		0.900	0.900	0.910
0.75		0.875	0.875	0.890
0.70		0.850	0.850	0.870

B. CONTINUOUS VOLTAGE TRACKING

With ideal maximum-power tracking, closed-loop feedback is used to capture the maximum available energy from the array by continuously tracking the array maximum-power voltage. This is one means of dealing with the site and fill-factor dependencies described above. The degree of voltage movement required to obtain most of the available energy is important to the design of such a system. This voltage window is most easily characterized by the center voltage in the window and the positive and negative percentage of movement, or tracking range from the center voltage.

The hourly computer simulations were used to develop data on the optimum center voltage and the fraction of the available energy that is obtained as a function of the tracking range. As might be expected, the optimum center voltage is nominally the same as the optimum fixed voltage presented in Table 2. Using the data in Table 2 for the center voltage, Figure 13 illustrates the percentage of loss in annual available energy for Albuquerque as a function of the tracking-range half width (stated as a percentage of the optimum center voltage).

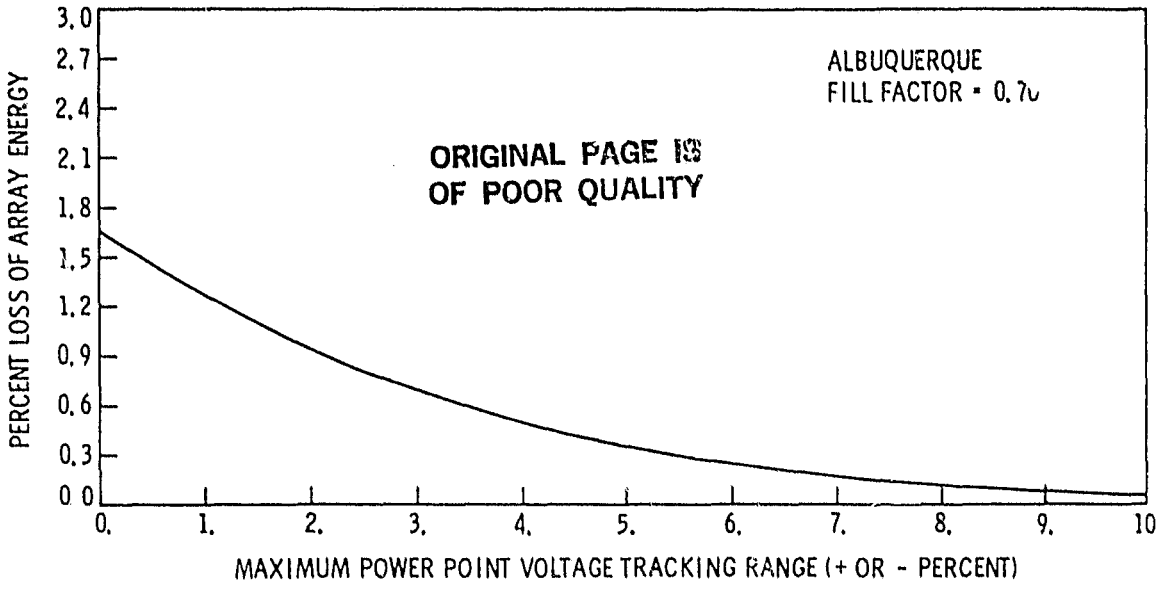

Figure 13. Percentage Loss in Annual Array Available Energy versus Power-Conditioner Voltage Tracking Range Half Width, Expressed as a Percentage of Optimum Center Voltage

Table 6 summarizes the key findings for the 26 sites analyzed with the following data:

(1) The optimum center voltage.

(2) The loss in available annual energy with ±5% voltage tracking.

(3) The voltage-tracking half width (percentage of the center voltage) required to obtain 99.9% of the available energy.

As these data show, a ±5% tracking range offers most of the available energy, and a ±12% tracking range is the maximum needed at any site.

Table 7 summarizes the modest effect of different fill factors on these results. The general trends are well in line with the ambient temperature and cloudy-day sensitivities noted previously.

An important consideration in the selection of continuous tracking as a strategy, and tracking range as a parameter, is the opportunity to accommodate not only the seasonal weather variations but also the site and fill-factor dependencies as well. The latter requires a tracking range that reflects the changing center voltage as well as the tracking range shown. From an analysis of the data in Table 7, it appears that a ±15% tracking width together with a center voltage around 0.95 will accommodate all of the 26 sites studied.

Before conclusions can be drawn about optimum tracking range, additional considerations must be made. These include the need for tracking to accommodate worst-case voltage, current and power levels, and the influence of long-term degradation of the array I-V curve shape.

Table 6. Simulation Results for Continuous-Tracking Power Conditioner

Site	Tracking Power-Conditioner Optimum Center Voltage (V_{op}/V_{maxp} at SOC)	% Loss In Energy With Power Conditioner With ± 5% Voltage Tracking	Tracking Required to Cut Energy Loss to 0.1% (± Percentage)
Albuquerque	0.96	0.35	8.5
Apalachicola	0.94	0.20	7.0
Bismarck	0.97	0.86	12.5
Boston	0.97	0.57	10.5
Brownsville	0.92	0.14	6.0
Cape Hatteras	0.95	0.31	8.5
Caribou	1.00	0.65	11.0
Charleston	0.95	0.20	7.0
Columbia	0.96	0.57	11.0
Dodge City	0.95	0.50	10.0
El Paso	0.94	0.22	7.0
Ely	0.98	0.36	8.0
Fort Worth	0.93	0.35	9.0
Fresno	0.94	0.21	7.0
Great Falls	0.97	0.58	11.5
Lake Charles	0.93	0.25	8.0
Madison	0.97	0.72	12.0
Medford	0.96	0.28	8.0
Miami	0.93	0.12	5.5
Nashville	0.95	0.45	10.0
New York	0.97	0.45	10.0
Omaha	0.96	0.64	12.0
Phoenix	0.92	0.25	7.5
Santa Maria	0.97	0.10	5.0
Seattle	0.97	0.31	8.0
Sterling	0.96	0.40	9.0

ORIGINAL PAGE IS
OF POOR QUALITY

ORIGINAL PAGE IS
OF POOR QUALITY

Table 7. Sensitivity of Continuous-Tracking Parameters to Array Fill Factor

Site	Fill Factor	Optimum Operating Voltage	Tracking Required to Cut Energy Loss to 0.1% (± Percentage)
Albuquerque	0.45	0.90	11.0
	0.50	0.91	11.5
	0.55	0.93	11.5
	0.60	0.94	12.0
	0.65	0.95	11.0
	0.70	0.96	8.5
	0.75	0.96	8.0
Bismarck	0.45	0.88	14.0
	0.50	0.90	15.0
	0.55	0.93	16.0
	0.60	0.95	16.0
	0.65	0.96	15.5
	0.70	0.97	12.5
	0.75	0.99	11.0
Boston	0.45	0.85	11.0
	0.50	0.88	12.0
	0.55	0.90	12.0
	0.60	0.92	13.0
	0.65	0.94	13.0
	0.70	0.97	10.5
	0.75	0.99	7.5
Miami	0.45	0.80	6.0
	0.50	0.83	6.5
	0.55	0.86	7.0
	0.60	0.88	7.5
	0.65	0.90	5.5
	0.70	0.93	5.5
	0.75	0.95	3.0
Phoenix	0.45	0.85	8.0
	0.50	0.87	8.5
	0.55	0.89	9.0
	0.60	0.90	9.0
	0.65	0.91	9.0
	0.70	0.92	7.5
	0.75	0.92	7.0

ORIGINAL PAGE IS
OF POOR QUALITY

Another consideration in the design of voltage tracking systems is the degree to which the control algorithm leads to local searching or oscillation about the maximum power point. This problem is aggravated by the continuous and often rapid motion of the array maximum power point due to ever-present fluctuations in the solar irradiance level. Temperature changes, on the other hand, generally vary slowly, with time constants ranging from 2 to 10 minutes.

Depending on the amplitude of oscillation about the maximum power point, sufficient energy can be lost to negate the advantages of continuous tracking. Figure 14 illustrates the fraction of available energy that is lost as a function of the peak amplitude of a sinusoidal voltage oscillation about the maximum power point. Figure 14 was constructed by assuming a sinusoidal variation in the voltage and computing array power loss.

This relationship applies equally to the presence of ripple fed back onto the array from a power-conditioner inverter. The switching within a 60-Hz inverter can generate a ripple current on the array that effectively changes the array operating voltage 120 times per second. The extent and duration of this voltage change, which forces the array off its maximum power operating point, will result in a net energy loss.*

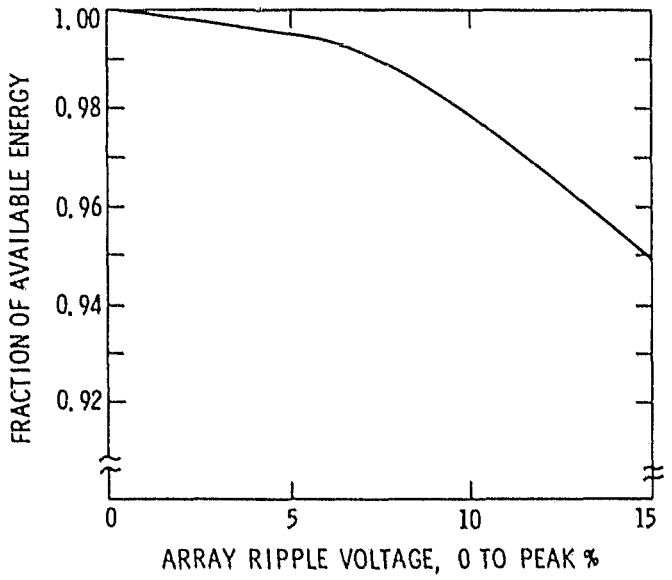

Figure 14. Effect of Sinusoidal Ripple on Array Energy Output

*Inverter-induced ripple current can be reduced significantly by adding a reactive component to the dc bus. A shunt capacitor is used for a voltage-sourced inverter and a series inductor is used for a current-sourced inverter. The size of this reactive component determines ripple reduction. In any ac photovoltaic system a large reactive component is required to balance the dc-to-ac energy flow by matching the constant array output power instantaneously with the varying power conditioner output power. The reactive requirement for energy balance is normally sufficient to negate the ripple effects on maximum-power-point operation.

SECTION IV

ESTABLISHING MAXIMUM OPERATING LIMITS

Another important power-conditioner design issue is the maximum power, current and voltage that the power conditioner must be capable of withstanding. At least three key considerations are evident:

(1) The amount of energy that is lost during times when the array output exceeds PCS operating limits and energy is rejected.

(2) The protection strategy to be implemented when the maximum limits are exceeded.

(3) The absolute maximum levels expected if survival limits are a consideration.

A. CURRENT AND POWER LIMITS

A key consideration in the selection of current and power limits is the cost of accepting higher levels compared with the energy lost or down-time suffered when over-limit conditions are encountered. At least three basic protection strategies exist. One involves PCS shutdown, with manual reset, when ratings are exceeded. This operating strategy requires that operating limits be set near the maximum foreseeable values in order to eliminate nuisance tripping. A second strategy involves total rejection of power during overlimit conditions, with automatic recovery when acceptable levels return. The third strategy involves rejection of only enough power to bring the current or power within limits. This strategy could be accomplished by shunting some of the array current around the PCS or by moving away from the maximum power point to a location on the I-V curve with acceptable power and current levels.

To assess the above options the energy loss was calculated for the last two strategies as a function of the PCS current and power levels. In addition the maximum foreseeable current and power levels were estimated to guide the manual-reset option.

Figures 15 and 16 show the fraction of available annual energy obtained at Albuquerque as a function of the current and power limits, assuming the two strategies: total rejection of power when limits are exceeded, followed by automatic reset, and rejection of only that power necessary to achieve operation within the limits. Table 8 summarizes the power and current limits that would result in obtaining 99% and 99.9% of the available annual energy for the 26 sites examined. In each case, the limits are normalized to the array maximum power and current at maximum power at SOC.

For the operational mode that totally rejects power during over-limit conditions, the current and power limits required to obtain 99% of the available energy average about 7% greater than the array SOC values. In contrast, for the operational mode in which only excess power is rejected, the power and current limits required to obtain 99% of the available energy

PAGE 24 INTENTIONALLY BLANK

PRECEDING PAGE BLANK NOT FILMED

ORIGINAL PAGE IS
OF POOR QUALITY

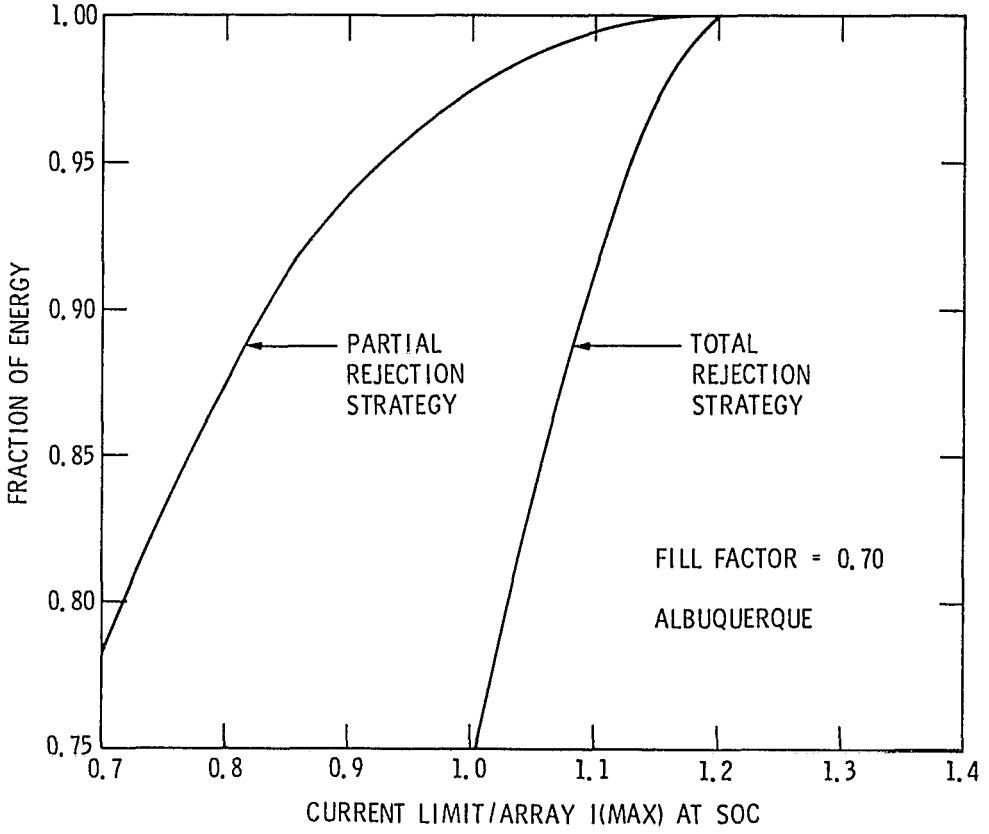

Figure 15. Fraction of Annual Array Energy Obtained versus PCS Input-Current Limit for Two Over-Limit Current-Management Strategies

average about 8% below the array SOC values. This implies that, on the average, for the same energy performance, a power conditioner using a total rejection strategy must accommodate levels about 15% higher than a power conditioner using a partial rejection strategy.

For the partial rejection strategy, it is also useful to know the maximum voltage excursion away from the power-conditioner center voltage that would be required to bring the operating levels within the limits. This was determined for a power conditioner sized to obtain 99.9% of the available energy, and is included in the last column of Table 8. It shows that the maximum excursion ranges from 5% to 17% of the center voltage, and exceeds the tracking-range requirements presented in Table 3, which assumed no current or power limits.

In order to limit the complexity and cost of the computer analyses performed, the maximum limits for each parameter were determined independently of each other. For example, the maximum voltage tracking width required to reduce the over-current (to that value of current required to obtain 99.9% of the array energy) will be different from the voltage tracking width required to obtain 99.9% of the energy without regard to current, and is determined separately. The justification for considering these two voltage limits separately is that a PCS may operate with voltage power tracking and use a strategy for limiting current other than a voltage excursion on the array I-V

ORIGINAL PAGE IS
OF POOR QUALITY

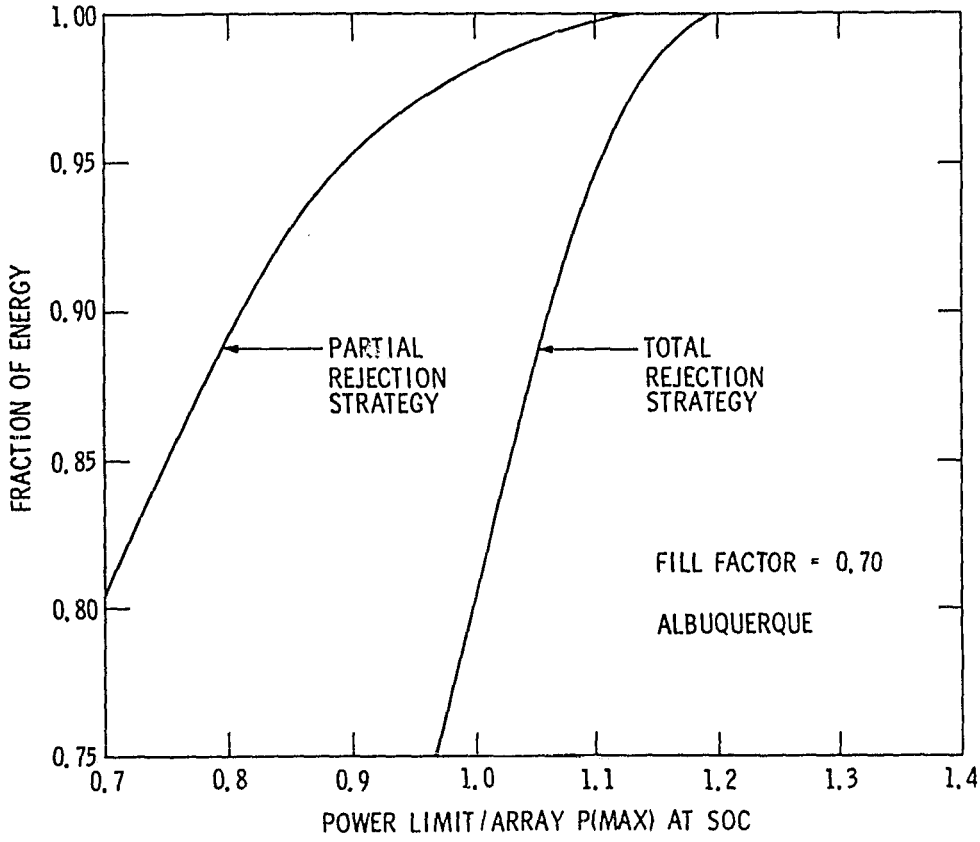

Figure 16. Fraction of Annual Energy Obtained versus PCS Input-Power Limit for Two Over-Limit Power-Management Strategies

curve. In a PCS using both voltage power tracking and voltage excursion to limit current, the latter may be used to define the voltage tracking width independently of any other consideration.

The small effect of fill factor on the maximum current and power limits is illustrated in Table 9.

For some design tradeoffs, data on the absolute maximum power and current levels may also be of interest. These maxima will generally be reached under circumstances of clear, cold days together with enhanced radiation from white clouds, snow, sand, water, white buildings or other reflecting surfaces near the array. Because the degree of enhancement is highly site-dependent, only the broadest guidance can be provided. In general, irradiance levels, and thus current levels, 1.3 times the SOC values are the maximum seen without abnormal enhancement from ground-based reflecting surfaces. The effect of ground-based reflectors such as snow or white buildings is very geometry-sensitive with increases perhaps as much as 30% possible under unusual circumstances.

Table 8. Effect of Partial and Total Rejection Strategies on Power and Current Limits versus Fraction of Available Energy Obtained

Site	$\left(\frac{\text{PC Power Limit}}{\text{Array Power at SOC}}\right)$ to Gain 99% of Energy Obtained With No Limit		$\left(\frac{\text{PC Power Limit}}{\text{Array Power at SOC}}\right)$ to Gain 99.9% of Energy Obtained With No Limit		$\left(\frac{\text{PC Current Limit}}{\text{Array } I_{maxp} \text{ at SOC}}\right)$ to Gain 99% of Energy Obtained With No Limit		$\left(\frac{\text{PC Current Limit}}{\text{Array } I_{maxp} \text{ at SOC}}\right)$ to Gain 99.9% of Energy Obtained With No Limit		Voltage Excursion from Center for 99.9% Limit, %
	Partial	Total	Partial	Total	Partial	Total	Partial	Total	
Albuquerque	1.04	1.15	1.13	1.19	1.06	1.19	1.17	1.20	11.5
Apalachicola	0.86	1.02	0.99	1.06	0.91	1.03	1.01	1.06	5.3
Bismarck	0.96	1.11	1.08	1.15	0.95	1.07	1.05	1.10	15.5
Boston	0.89	1.06	1.02	1.11	0.89	1.04	1.01	1.09	13.4
Brownsville	0.85	1.02	0.97	1.06	0.92	1.04	1.03	1.05	6.5
Cape Hatteras	0.89	1.06	1.03	1.10	0.92	1.06	1.03	1.09	14.7
Caribou	0.98	1.15	1.14	1.24	0.94	1.09	1.08	1.10	15.0
Charleston	0.87	1.03	1.00	1.09	0.90	1.04	1.01	1.08	9.5
Columbia	0.95	1.12	1.09	1.15	0.95	1.08	1.06	1.10	15.6
Dodge City	1.00	1.14	1.12	1.20	1.01	1.17	1.12	1.20	10.5
El Paso	1.01	1.12	1.10	1.15	1.03	1.17	1.15	1.20	9.6
Ely	1.05	1.17	1.15	1.23	1.05	1.19	1.16	1.20	9.2
Fort Worth	0.91	1.06	1.04	1.10	0.94	1.05	1.04	1.10	15.1
Fresno	0.92	1.04	1.03	1.07	0.98	1.05	1.04	1.05	10.6
Great Falls	0.94	1.09	1.07	1.16	0.96	1.06	1.05	1.10	15.5
Lake Charles	0.84	0.93	0.92	1.06	0.86	0.95	0.94	0.96	17.2
Madison	0.98	1.18	1.15	1.32	0.95	1.10	1.09	1.19	15.5
Medford	0.90	1.07	1.05	1.10	0.94	1.07	1.05	1.10	8.3
Miami	0.82	0.92	0.91	1.03	0.86	1.02	0.97	1.05	9.7
Nashville	0.89	1.06	1.03	1.11	0.91	1.06	1.03	1.09	14.7
New York	0.88	1.07	1.03	1.13	0.88	1.00	0.99	1.09	15.5
Omaha	0.97	1.12	1.10	1.21	0.95	1.09	1.08	1.26	12.5
Phoenix	0.93	1.06	1.05	1.10	1.00	1.06	1.05	1.16	9.8
Santa Maria	0.91	1.04	1.03	1.06	0.93	1.04	1.03	1.06	6.2
Seattle	0.86	0.94	0.93	1.05	0.88	0.95	0.95	0.96	12.4
Sterling	0.89	1.07	1.03	1.10	0.90	1.05	1.01	1.09	14.6

ORIGINAL PAGE IS
OF POOR QUALITY

Table 9. Effect of Array Fill Factor on Power and Current Limits Required to Obtain Various Fractions of Available Energy (Partial Rejection Strategy)

Site	Fill Factor	Power and Current Limits Required to Obtain Given Percentage of Energy			
		Power		Current	
		99%	99.9%	99%	99.9%
Albuquerque	0.45	1.06	1.17	1.06	1.14
	0.50	1.05	1.15	1.05	1.14
	0.55	1.04	1.13	1.05	1.14
	0.60	1.05	1.13	1.05	1.17
	0.65	1.04	1.13	1.04	1.14
	0.70	1.04	1.13	1.06	1.17
	0.75	1.04	1.13	1.06	1.17
Bismarck	0.45	0.98	1.11	0.96	1.07
	0.50	0.97	1.09	0.96	1.06
	0.55	0.97	1.09	0.96	1.04
	0.60	0.96	1.09	0.95	1.04
	0.65	0.96	1.09	0.95	1.05
	0.70	0.96	1.08	0.95	1.05
	0.75	0.96	1.07	0.95	1.05
Boston	0.45	0.90	1.04	0.91	1.01
	0.50	0.90	1.04	0.91	1.01
	0.55	0.90	1.04	0.91	1.01
	0.60	0.89	1.02	0.90	1.00
	0.65	0.89	1.02	0.90	1.00
	0.70	0.89	1.02	0.89	1.01
	0.75	0.90	1.01	0.89	1.01
Miami	0.45	0.83	0.91	0.87	0.98
	0.50	0.83	0.91	0.87	0.98
	0.55	0.82	0.91	0.86	0.98
	0.60	0.83	0.91	0.86	0.98
	0.65	0.82	0.91	0.86	0.97
	0.70	0.82	0.91	0.86	0.97
	0.75	0.85	0.95	0.86	0.97
Phoenix	0.45	0.93	1.05	1.00	1.06
	0.50	0.93	1.05	1.00	1.06
	0.55	0.93	1.04	1.00	1.05
	0.60	0.93	1.05	1.00	1.05
	0.65	0.93	1.05	1.00	1.05
	0.70	0.93	1.05	1.00	1.05
	0.75	0.95	1.04	1.00	1.06

B. VOLTAGE LIMITS

Voltage limits must also be considered by the PCS design, particularly during startup when the array may be at its maximum open-circuit voltage. Worst-case open-circuit voltages generally are associated with low temperatures and high irradiance levels, such as might be encountered during a bright, cold winter day with snow on the ground. Three approaches were used to estimate likely maximum open-circuit voltages:

(1) The hourly combination of incident irradiance and calculated cell temperature (based on incident irradiance and ambient air temperature) that led to the maximum open-circuit voltage was noted. This voltage represents the worst-case thermal equilibrium condition existing on the SOLMET TMY tape. Because this condition does not reflect the easily foreseeable case where the sun suddenly appears from behind an obstruction and shines on a cold array, it is considered to be a lower-bound estimate of the maximum open-circuit voltage.

(2) The coldest ambient temperature as recorded in the SOLMET TMY data tape was assumed as the solar-cell temperature. This cell temperature was then combined with a 100 mW/cm^2 solar irradiance level to determine the array open-circuit voltage at these conditions. Since the simultaneous occurrence of such conditions is unlikely, this determination of open-circuit voltage can be viewed as an upper limit for the selected TMY.

(3) The coldest ambient temperature as recorded in a weather atlas (Reference 3) was assumed as the solar-cell temperature for each site. This cell temperature was then combined with a 100 mW/cm^2 solar irradiance level to determine the array open-circuit voltage at these conditions. This condition is considered to yield a true upper-bound value because of the inclusion of long-term weather extremes.

Table 10 summarizes the results from the three estimating techniques. Because the upper-bound estimates are only about 12% higher than the lower-bound estimates, they serve as a useful basis for estimating the worst-case voltages for any site without suffering an excessive penalty for conservatism. Figure 17 gives a plot of the results in Column 2 against Column 3. This provides an indication of how well the upper bound obtained from the TMY tape correlates with that obtained from an atlas.

To further generalize these worst-case-voltage estimates, it is useful to consider explicitly the effect of two key design parameters: the effect of changing NOCT and the effect of changing fill factor. Although NOCT has no effect on the maximum array voltage, which is based solely on coldest ambient temperature, it directly affects the maximum-power voltage at SOC to which the maximum voltages are normalized. As a result the normalized maximum open-circuit voltage increases at a rate of about 0.5% per ^{o}C rise in NOCT above the baseline value of 50^{o}C used in Table 10.

ORIGINAL PAGE IS
OF POOR QUALITY

Table 10. Estimated Maximum Open-Circuit Voltage for 26 Sites (NOCT = 50°C)

Site	Maximum Open-Circuit Voltage V_{maxp} at SOC		
	Lower Bound from TMY*	Upper Bound from TMY	Upper Bound from Atlas
Albuquerque	1.49	1.69	1.74
Apalachicola	1.43	1.62	1.64
Bismarck	1.57	1.79	1.83
Boston	1.52	1.69	1.69
Brownville	1.43	1.57	1.57
Cape Hatteras	1.46	1.63	1.63
Caribou	1.57	1.79	1.82
Charleston	1.46	1.64	1.65
Columbia	1.55	1.74	1.74
Dodge City	1.52	1.71	1.73
El Paso	1.46	1.65	1.71
Ely	1.55	1.76	1.77
Fort Worth	1.46	1.66	1.67
Fresno	1.44	1.61	1.61
Great Falls	1.57	1.77	1.83
Lake Charles	1.46	1.64	1.64
Madison	1.57	1.79	1.81
Medford	1.49	1.66	1.69
Miami	1.40	1.56	1.56
Nashville	1.53	1.67	1.72
New York	1.50	1.69	1.69
Omaha	1.58	1.75	1.75
Phoenix	1.43	1.61	1.61
Santa Maria	1.40	1.61	1.61
Seattle	1.49	1.64	1.64
Sterling	1.52	1.71	1.71

*Startup voltage for 99.9% of available annual energy

ORIGINAL PAGE IS
OF POOR QUALITY

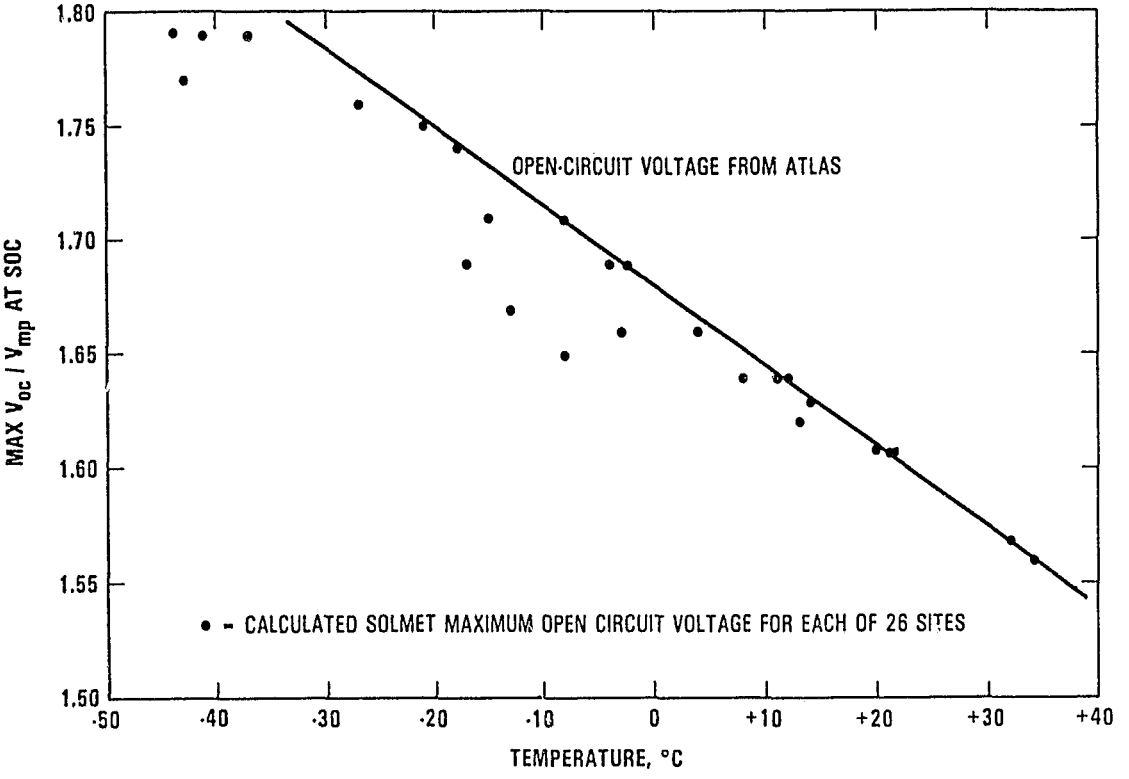

Figure 17. Maximum Open-Circuit Voltage (from SOLMET TMY) versus Atlas Lowest Recorded Temperature

The following empirical equation includes the observed influences of NOCT and fill factor and allows rapid calculation of the normalized maximum open-circuit voltage for any site in terms of its coldest temperature (T_L):

$$\frac{\text{Maximum } V_{oc}}{V_{maxp} \text{ at SOC}} = 0.475\ (2\text{-FF})\ (1 - \alpha T_L)\ (2 + \frac{\text{NOCT}}{100}) \qquad (1)$$

where

FF = fill factor of array

T_L = coldest ambient temperature, °C

NOCT = nominal operating cell temperature, °C

α = fractional change in the open-circuit voltage at 25°C for each degree of change in temperature, °C

It should be noted that open-circuit voltage moves more slowly with temperature than does the knee of the I-V curve and leads to values of α ranging from 0.003 to 0.004. The baseline analysis displayed in Table 10 used the maximum, but often-encountered, value of 0.004.

Although accommodation of the maximum open-circuit voltage will be a requirement for most power-conditioner designs, the maximum withstandable voltage could be limited to the non-operating state. In this case, power-conditioner startup would not occur unless the array open-circuit voltage were below some allowable start-up voltage limit. Examination of the detailed simulation results indicates that the lower-bound estimates in Table 10 are a good selection for a startup-voltage limit with minimal energy loss. With a PCS startup-voltage limit at or above these values, less than 0.1 % energy loss is suffered; below these values the energy loss increases rapidly.

ORIGINAL PAGE IS
OF POOR QUALITY

SECTION V

COMPUTING SYSTEM EFFICIENCY

An additional aspect of long-term array performance that is important to the design of array-loading systems is the fraction of annual energy generated at various power levels. This information is particularly useful in quantifying the annual energy losses associated with power conditioner internal efficiency. Because power-conditioner efficiency typically varies with output power level, the calculation of average efficiency (or total annual energy losses) requires data on the fraction of annual energy input to the PCS as a function of power level.

The hourly simulation results for the 26 sites were used to construct plots defining the operating time, and thus the annual energy generated, at various relative power levels. To help understand the data presentation format it is useful first to consider a typical plot of power output versus time for a period of one day. Such a plot, illustrated on the left in Figure 18, can be modified in a useful way by rearranging the hourly intervals in order of decreasing power output level as shown at the right in Figure 18. Figure 19 is the result of performing the same operation on the hourly computer simulation results for an entire year for Albuquerque. Such a plot is useful in that the area under the curve is the annual energy output (integral of power over time) and the area under any two power levels is the energy generated during operation between these levels. The shaded area of Figure 19 thus equals the total energy generated at power levels between zero and 50% of the array maximum power at SOC.

Table 11 tabulates the fraction of annual energy generated within each of 12 power intervals for each of the 26 sites. The fractions serve as useful

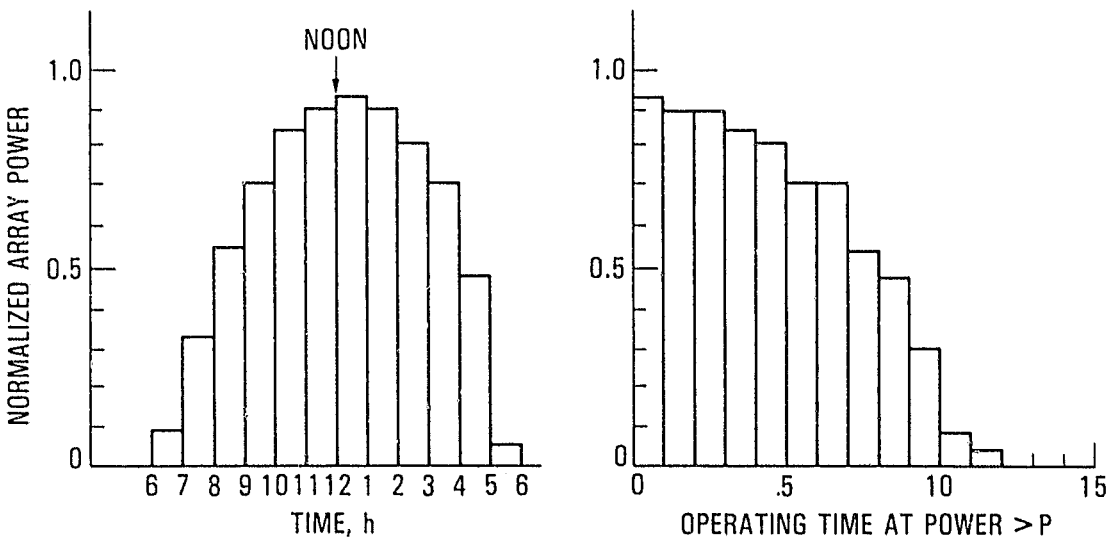

Figure 18. Illustration of the Construction Principle Behind a Plot of Normalized Power versus Operating Time With the Time Intervals Ordered According to Decreasing Power Level

PRECEDING PAGE BLANK NOT FILMED

PAGE 34 INTENTIONALLY BLANK

ORIGINAL PAGE IS
OF POOR QUALITY

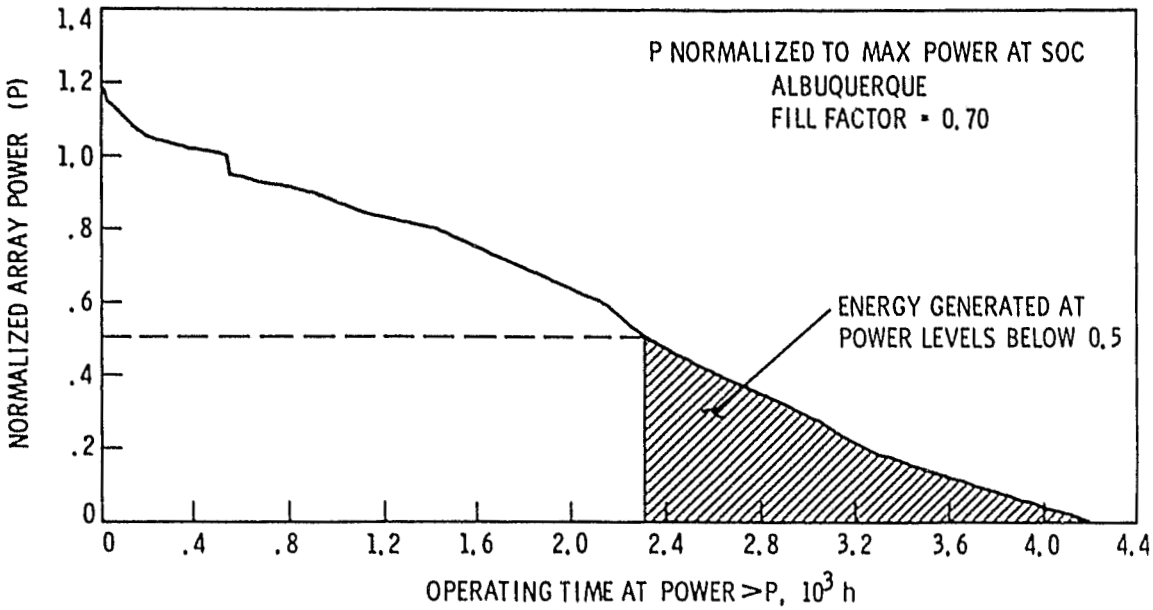

Figure 19. Hours of Array Operation versus Array Power Level During One Year

weighting factors for the determination of an average power-conditioner efficiency, which is defined as annual energy output to the load divided by the annual energy input to the PCS.

Mathematically this definition can be expressed as:

$$\eta_{ave} = \frac{\int P_{out}\, dt}{\int P_{in}\, dt} = \frac{\int \eta_{(P_{in})}\, P_{in}\, dt}{\int P_{in}\, dt} \qquad (2)$$

where

P_{in} = input power to PCS

P_{out} = output power from PCS

$\eta_{(P_{in})}$ = PCS efficiency expressed as a function of P_{in}

If we approximate the integrals with summations over N distinct power intervals (P1 through PN) we obtain:

$$\eta_{ave} = \left[\left(K_1 \sum_{P=P1}^{PN} \eta_P\, E_P\right) - P_{SB}\, T_{SB}\right] \Bigg/ \sum_{P=P1}^{PN} E_P \qquad (3)$$

or

$$\eta_{ave} = K_1 \left(\sum_{P=P1}^{PN} \eta_P\, \frac{E_P}{E_y}\right) - \frac{R_{SB}\, R\, \eta_1 T_{SB}}{(E_y/P_{max})} \qquad (4)$$

Table 11. Fraction of Annual Array Energy Available in Various Relative Power Intervals for 26 Sites

Site	Array Relative Power Interval											
	0-0.1	0.1-0.2	0.2-0.3	0.3-0.4	0.4-0.5	0.5-0.6	0.6-0.7	0.7-0.8	0.8-0.9	0.9-1.0	1.0-1.1	1.1-1.2
Albuquerque	0.0079	0.0264	0.0274	0.0508	0.0488	0.0552	0.0959	0.1174	0.1849	0.1844	0.1499	0.0511
Apalachicola	0.0120	0.0401	0.0479	0.0849	0.0557	0.1117	0.1632	0.2126	0.2135	0.0430	0.0155	0.0000
Bismarck	0.0221	0.0529	0.0594	0.0769	0.0560	0.0882	0.1097	0.1338	0.2296	0.0976	0.0607	0.0132
Boston	0.0331	0.0576	0.0563	0.0820	0.0724	0.1241	0.1308	0.1532	0.1880	0.0861	0.0147	0.0016
Brownsville	0.0133	0.0439	0.0467	0.0926	0.0468	0.1557	0.1899	0.2068	0.1549	0.0356	0.0138	0.0000
Cape Hatteras	0.0175	0.0456	0.0478	0.0795	0.0601	0.1008	0.1404	0.2056	0.2119	0.0689	0.0212	0.0007
Caribou	0.0222	0.0557	0.0866	0.0868	0.1057	0.0697	0.1281	0.1230	0.1564	0.0978	0.0277	0.0412
Charleston	0.0115	0.0426	0.0556	0.0956	0.0738	0.1258	0.1810	0.1939	0.1480	0.0563	0.0158	0.0000
Columbia	0.0212	0.0496	0.0475	0.0734	0.0547	0.1008	0.1288	0.1432	0.2270	0.0888	0.0494	0.0154
Dodge City	0.0145	0.0372	0.0391	0.0606	0.0426	0.0758	0.1165	0.1258	0.2317	0.1474	0.0812	0.0275
El Paso	0.0051	0.0262	0.0259	0.0554	0.0369	0.0779	0.1011	0.1485	0.2128	0.1713	0.1172	0.0217
Ely	0.0062	0.0258	0.0394	0.0586	0.0623	0.0787	0.0891	0.1010	0.1936	0.1477	0.1307	0.0670
Fort Worth	0.0181	0.0409	0.0497	0.0688	0.0505	0.1137	0.1416	0.1768	0.2150	0.0845	0.0391	0.0012
Fresno	0.0097	0.0349	0.0435	0.0555	0.0519	0.0694	0.1242	0.1479	0.2944	0.1154	0.0511	0.0022
Great Falls	0.0207	0.0504	0.0553	0.0772	0.0686	0.0864	0.1237	0.1402	0.2129	0.1002	0.0573	0.0072
Lake Charles	0.0190	0.0507	0.0587	0.0990	0.0650	0.1545	0.1865	0.1998	0.1405	0.0235	0.0026	0.0000
Madison	0.0255	0.0552	0.0618	0.0778	0.0671	0.1020	0.1092	0.1674	0.1690	0.0898	0.0416	0.0319
Medford	0.0227	0.0538	0.0518	0.0815	0.0535	0.1036	0.1112	0.1346	0.2699	0.0856	0.0309	0.0007
Miami	0.0105	0.0403	0.0622	0.0932	0.0803	0.1579	0.2439	0.2009	0.0901	0.0172	0.0035	0.0000
Nashville	0.0246	0.0526	0.0606	0.0726	0.0597	0.1253	0.1624	0.1891	0.1600	0.0700	0.0208	0.0022
New York	0.0239	0.0501	0.0670	0.0780	0.0951	0.1076	0.1383	0.1798	0.1671	0.0774	0.0132	0.0025
Omaha	0.0204	0.0478	0.0514	0.0768	0.0515	0.0911	0.1201	0.1522	0.2094	0.1025	0.0593	0.0174
Phoenix	0.0084	0.0255	0.0343	0.0536	0.0442	0.0833	0.1109	0.1982	0.2575	0.1246	0.0581	0.0015
Santa Maria	0.0128	0.0330	0.0352	0.0635	0.0400	0.0935	0.0843	0.1794	0.3242	0.0898	0.0443	0.0000
Seattle	0.0410	0.0892	0.0726	0.0877	0.0723	0.1124	0.0759	0.1765	0.2172	0.0520	0.0032	0.0000
Sterling	0.0190	0.0507	0.0714	0.0865	0.0734	0.1224	0.1481	0.1694	0.1623	0.0769	0.0182	0.0015
Average	0.0178	0.0453	0.0521	0.0757	0.0611	0.1034	0.1329	0.1645	0.2016	0.0898	0.0439	0.0118
Cumulative Value of Averages	0.0178	0.0631	0.1152	0.1909	0.2520	0.3554	0.4883	0.6528	0.8544	0.9442	0.9881	1.0000

ORIGINAL PAGE IS
OF POOR QUALITY

ORIGINAL PAGE IS
OF POOR QUALITY

where

K_1 = fraction of array available annual energy obtained at the PCS input (K_1 = 1 for ideal max power tracking; K_1 is obtained from Table 2 for fixed-voltage operation, and other values may be obtained for limited tracking from Table 3)

E_P = annual PCS input energy in array power interval P

E_y = total annual input energy = $\sum_{P=P1}^{PN} E_P$

$\frac{E_p}{E_y}$ = fraction of annual array energy available in array power interval P; obtained from Table 11

P_{SB} = standby PCS power consumption per hour

T_{SB} = hours per year for which PCS has no output power, but draws standby power

R_{SB} = P_{SB}/PCS full-output-power rating

η_P = PCS efficiency for input-power interval P

η_1 = PCS efficiency at PCS full-power rating

R = ratio of PCS full-input-power rating to array maximum power at SOC

= ratio of (PCS full-output-power rating divided by η_1) to array maximum power at SOC

P_{max} = array maximum power at SOC

E_y/P_{max} = total annual electrical energy per unit of array power at SOC; this is very accurately approximated by the number of kWh/m^2/year of incident irradiance captured by the array at the site of interest; a value typically between 1500 and 2500

Because power-conditioner efficiencies are sometimes quoted in terms of PCS output power level, it is important to note that Equation (4) requires efficiency in terms of array power level, to be compatible with the array power intervals used to evaluate the (E_P/E_y) terms that are tabulated in Table 11. Figure 20 illustrates a typical power-conditioner efficiency curve presented as a function of a fraction of PCS full-output-power rating. To obtain the required curve in terms of array relative power requires that each of the efficiency points be translated horizontally to a new relative power location defined by:

$$\left(\frac{\text{Array power at } \eta_P}{\text{Maximum power at SOC}}\right) = \left(\begin{matrix}\text{PCS relative}\\ \text{output power}\\ \text{at } \eta_P\end{matrix}\right)\left(\frac{\eta_1 R}{\eta_P}\right) \qquad (5)$$

ORIGINAL PAGE IS
OF POOR QUALITY

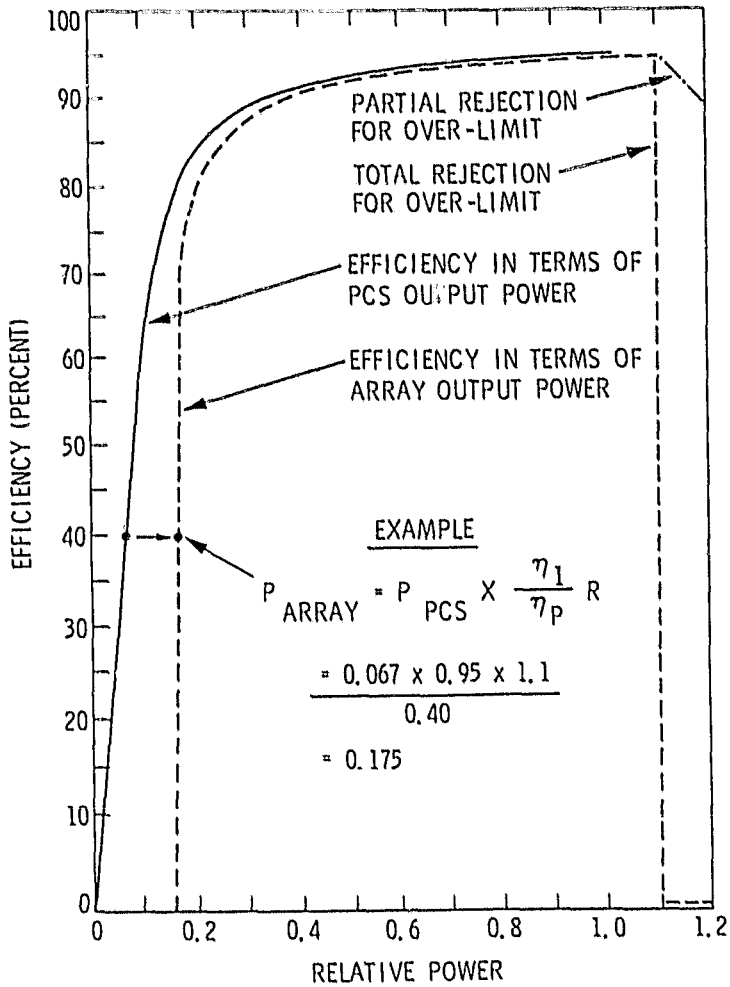
EFFICIENCY (PERCENT)
RELATIVE POWER
PARTIAL REJECTION FOR OVER-LIMIT
TOTAL REJECTION FOR OVER-LIMIT
EFFICIENCY IN TERMS OF PCS OUTPUT POWER
EFFICIENCY IN TERMS OF ARRAY OUTPUT POWER
EXAMPLE
P ARRAY = P PCS X η1/ηP R
= 0.067 x 0.95 x 1.1 / 0.40
= 0.175

Figure 20. Typical Power-Conditioner Efficiency vs Fraction of Power-Conditioner Full-Output Power Rating and Array Maximum Power at SOC

In the above equation the term η_1/η_P converts the PCS relative output power to PCS relative input power; the R term then converts the PCS relative input power to array relative output power, which is normalized in terms of array maximum power at SOC instead of PCS full-power rating.

The dashed line in Figure 20 illustrates the appropriately translated curve for the example power conditioner, assuming that it was sized to have a full-input-power rating of 1.1 times the array maximum power at SOC. At array relative-power levels above 1.1 the power conditioner efficiency is zero for the case where total shutdown occurs when the PCS limits are exceeded, and decreases as shown for the partial-rejection case, where only the power above the limit is rejected.

In the partial rejection case the average PCS efficiency (η_P) in the over-limit power intervals can be accurately approximated as:

$$\eta_P = \frac{\eta_1 \, R}{\bar{P}_P} \qquad (6)$$

where $\bar{P}_P$ is the average relative power in power interval P.

This expression together with the dashed curve in Figure 20 gives an average efficiency value η_p for each of the 12 array power intervals defined in Table 11. These are tabulated in Table 12 for Albuquerque for both the total-rejection and partial-rejection over-limit control strategies, and also for two additional PCS-to-array power ratios (R = 1.0 and R = 1.2). Entering these values and the fraction-energy values (E_p/E_y) into Equation (4) gives the average annual efficiency values shown in Table 12 for each of the six example cases.

In order to obtain the results in Table 12 the following values were used:

K_1 = 0.983 (from Table 2 for fixed-voltage operation)

R_{SB} = 0.01 (assumed value)

T_{SB} = 5400 h (from Figure 21)

E_y/P_{max} = 2360 kWh/kW (the annual irradiance, kWh/m^2/year, for a south-facing, latitude-tilt surface in Albuquerque)

η_1 = 0.95 (from Figure 20)

The above assumptions give values for the second term in Equation 4 of 0.022, 0.024, and 0.026 respectively for the three pairs of columns in Table 12.

Two important points appear in Table 12:

(1) An optimum power-conditioner-to-array ratio (R) is established by the tradeoff between increased over-limit losses and higher below-limit efficiency as the size of the PCS is reduced. For the case of partial rejection of over-limit power, the optimum ratio (R) is 1.1 in this example. Note, however, that the optimum is quite flat, indicating a substantial tolerance to the size of the array or to the site location. A second tradeoff involves the cost of a higher power limit versus the loss in annual energy.

(2) The penalty for total rejection of over-limit power is very large, and essentially requires a PCS rating 20% larger than for partial rejection.

Figure 21 illustrates the power-conditioner losses on a reproduction of Figure 19.

Table 11 provides average values of E_p/E_y for the 26 sites analyzed. These values were used to derive a curve of normalized power versus operating time at a given power level or greater, as shown in Figure 22, which is similar to the example for Albuquerque given in Figure 19. Figure 22 is a composite curve representative of all 26 sites and the total time of operation, 4040 hours, is an average of all sites. Therefore Figure 22 represents the annual array power output profile for a site that characterizes the average for the United States.

Table 11 and Figure 22 may be used to calculate an average power-conditioner efficiency representative of any site in the United States. The

ORIGINAL PAGE IS
OF POOR QUALITY

Table 12. Example Average Annual Efficiency Calculation for Albuquerque

Relative Power Interval (P)	Annual Energy Fraction (E_P/E_y)	Average Power-Conditioner Efficiency in Power Interval (P)					
		R = 1.0		R = 1.1		R = 1.2	
		Total	Partial	Total	Partial	Total	Partial
0.0-0.1	0.0079	0	0	0	0	0	0
0.1-0.2	0.0264	0.300	0.300	0.180	0.180	0.060	0.060
0.2-0.3	0.0274	0.850	0.850	0.825	0.825	0.800	0.800
0.3-0.4	0.0508	0.900	0.900	0.890	0.890	0.880	0.880
0.4-0.5	0.0488	0.918	0.918	0.914	0.914	0.907	0.907
0.5-0.6	0.0552	0.928	0.928	0.925	0.925	0.920	0.920
0.6-0.7	0.0959	0.935	0.935	0.932	0.932	0.928	0.928
0.7-0.8	0.1174	0.938	0.938	0.936	0.936	0.933	0.933
0.8-0.9	0.1849	0.942	0.942	0.940	0.940	0.938	0.938
0.9-1.0	0.1844	0.948	0.948	0.943	0.943	0.941	0.941
1.0-1.1	0.1499	0	0.905	0.948	0.948	0.945	0.945
1.1-1.2	0.0511	0	0.826	0	0.909	0.948	0.948
Standby Power Consumption (neg. value)		0.022	0.022	0.024	0.024	0.026	0.026
		Average Annual Efficiency, %					
Full Max-Power Tracking		70.0	87.8	83.3	88.0	87.3	87.3
Fixed-Voltage Operation		68.8	86.3	81.8	86.5	85.8	85.8

ORIGINAL PAGE IS
OF POOR QUALITY

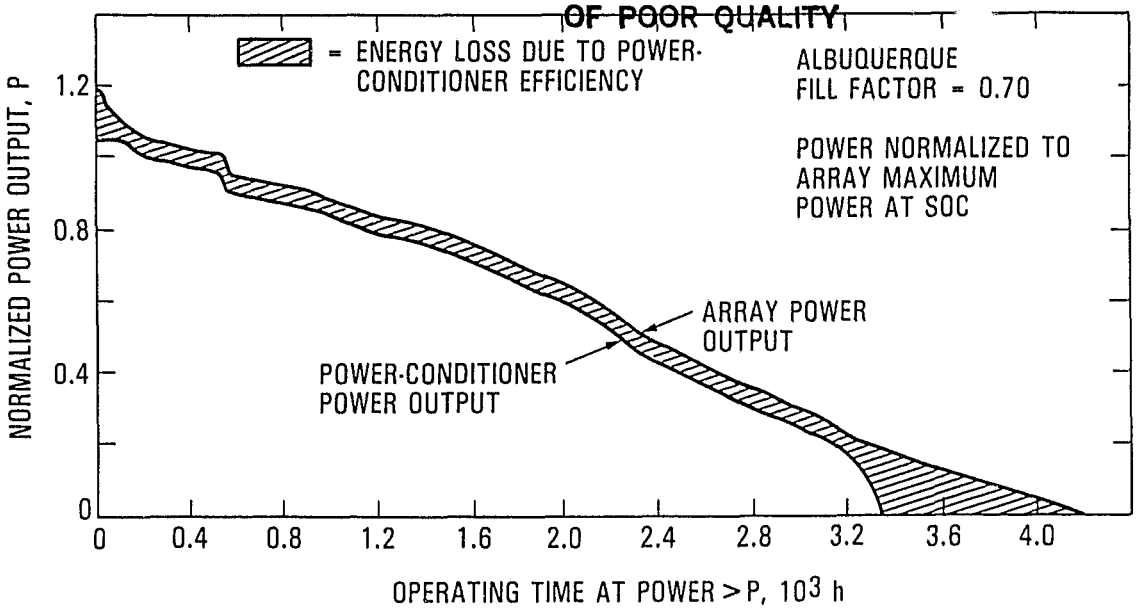

Figure 21. Effect of Typical Power-Conditioner Efficiency on Array Annual Power Production

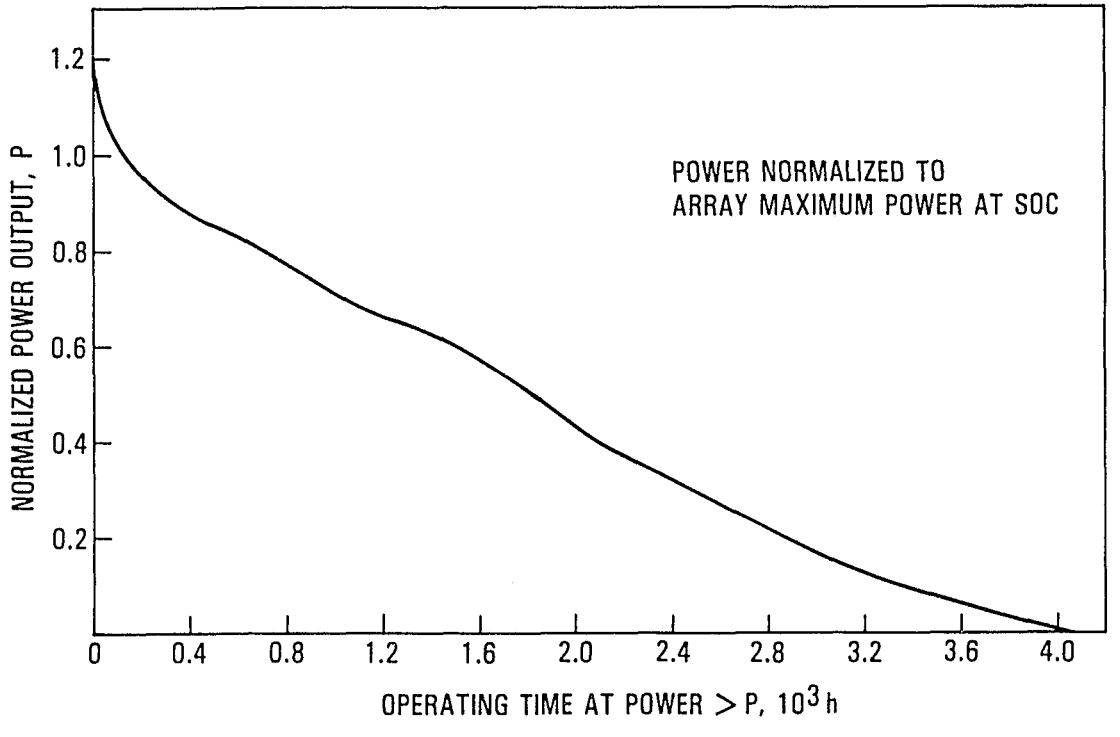

Figure 22. Composite of Annual Array Power Level versus Operating Hours for 26 Sites

following is a list of other average values that may be used to calculate average efficiency:

K_1 = 0.985 (obtained from Table 2)

T_{SB} = (in conjunction with the 2nd term in Equation 4) = 5800 h

E_y/P_{max} = (for sites similar to the following) (1) Boston, 1400 kWh/kW; (2) Bismarck, 1700 kWh/kW; (3) Dodge City, 2000 kWh/kW; (4) Albuquerque/Phoenix, 2360 kWh/kW

See the sample problem in the next section for more details.

SECTION VI

SAMPLE PROBLEM

To clarify and summarize use of the data previously presented, it is useful to treat an example problem. Consider determining the power conditioner interface parameters for a general purpose residential photovoltaic array specified by the manufacturer at 100 mW/cm^2, 25°C, as follows:

Maximum power	= 7.5 kW
Maximum power voltage	= 250 V
Maximum power current	= 30 A
Short circuit current	= 33 A
Fill factor	= 0.7

In the manufacturer's recommended roof-mounting configuration, the array is estimated to operate with an NOCT = 65°C.

To account for the influence of the actual operating temperature, the tabulated results in the report require that the array electrical performance be normalized to the estimated Standard Operating Conditions (100 mW/cm^2, 65°C). If design-specific array temperature coefficients are not provided by the manufacturer, we can assume the mean values presented in Table 1. Using these, we obtain the normalized SOC values as follows:

$$P_{max} \text{ at SOC} = 7.5\ [1 - 0.005\ (65)] = 6.0 \text{ kW}$$

$$V_{pmax} \text{ at SOC} = 250\ [1 - 0.005\ (65 - 25)] = 200 \text{ V}$$

$$I_{pmax} \text{ at SOC} = 30.0\ [1 + 0.0004\ (65 - 25)] = 30.5\text{A}$$

$$I_{sc} \text{ at SOC} = 33.0\ [1 + 0.0004\ (65 - 25)] = 33.5\text{A}$$

Assume next that it is desired to obtain typical power conditioner interface parameters based on average site conditions in the United States. Using the various average values tabulated throughout the report for the 26 SOLMET sites yields the results summarized in Table 13.

To estimate the average annual power conditioner efficiency, we use the average annual array energy fractions per power interval given in the bottom of Table 11. Table 14 presents the results based on these values and the following data required for the other terms in Equation 4:

$K_1 = 0.985$ (average from Table 2)

$\eta_1 = 0.95$ (assumed for power conditioner)

$R_{SB} = 0.01$ (assumed for power conditioner)

$T_{SB} = 5800$ h (from Figure 22)

$Ey/P_{max} = 1800$ kWh/kW (a seasonal average value for the United States)

PAGE 44 INTENTIONALLY BLANK

PRECEDING PAGE BLANK NOT FILMED

Table 13. Operating and Maximum Parameters

Parameter	Value	Source
PCS optimum fixed or optimum center voltage	190 V	Table 2 (average of all values in Col. 1) x 200 V
Voltage tracking range to obtain 99.9% of annual array energy	162-219 V	Table 6 (average of Col. 1 ± average of Col. 3) x 200 V
Highest startup V_{oc}	316 V	Table 10 (maximum value of Col. 1) x 200 V
Maximum expected V_{oc}	366 V	Table 10 (maximum values of Col. 3) x 200 V
Current limit required to obtain 99.9% of annual array energy with partial rejection strategy as described in the text	35.7 A	Table 8 (maximum value of Col. 7) x 30.5 A
Current limit required to obtain 99.9% of annual array energy with total rejection strategy as described in the text	38.4 A	Table 8 (maximum value of Col. 8) x 30.5 A
Maximum expected operating current	43.5 A	At least 1.3 I_{SC} at SOC (higher for special circumstances such as nearness to reflective surfaces, snow cover, high clouds, etc.)
Power limit required to obtain 99.9% of annual array energy with partial rejection strategy as described in the text	6.9 kW	Table 8 (maximum value of Col. 3) x 6 kW
Power limit required to obtain 99.9% of annual array energy with total rejection strategy as described in the text	7.9 kW	Table 8 (maximum value of Col. 4) x 6kW

ORIGINAL PAGE IS
OF POOR QUALITY

Table 14. Average Annual Efficiency Calculation for Composite of All 26 Sites

Relative Power Interval (P)	Annual Energy Fraction (E_p/E_y)	Average Power-Conditioner Efficiency in Power Interval (P)					
		R = 1.0		R = 1.1		R = 1.2	
		Total	Partial	Total	Partial	Total	Partial
0.0-0.1	0.0178	0	0	0	0	0	0
0.1-0.2	0.0453	0.300	0.300	0.180	0.180	0.060	0.060
0.2-0.3	0.0521	0.850	0.850	0.825	0.825	0.800	0.800
0.3-0.4	0.0757	0.900	0.900	0.890	0.890	0.880	0.880
0.4-0.5	0.0611	0.918	0.918	0.914	0.914	0.907	0.907
0.5-0.6	0.1034	0.928	0.928	0.925	0.925	0.920	0.920
0.6-0.7	0.1329	0.935	0.935	0.932	0.932	0.928	0.928
0.7-0.8	0.1645	0.938	0.938	0.938	0.936	0.933	0.933
0.8-0.9	0.2016	0.942	0.942	0.940	0.940	0.938	0.938
0.9-1.0	0.0898	0.948	0.948	0.943	0.943	0.941	0.941
1.0-1.1	0.0439	0	0.905	0.948	0.948	0.945	0.945
1.1-1.2	0.0118	0	0.826	0	0.909	0.948	0.948
Standby Power Consumption (neg. value)		0.031	0.031	0.034	0.034	0.037	0.037
		Average Annual Efficiency, %					
Full Max-Power Tracking		80.1	85.0	83.0	84.0	82.8	82.8
Fixed-Voltage Operation		78.9	83.7	81.8	82.7	81.6	81.6

SECTION VII

CONCLUSIONS

The information included in the above figures and tables should provide a useful data base for designing array loading systems that effectively utilize the output from a photovoltaic array. In addition, the summary of site-to-site and fill-factor influences should serve to identify capabilities needed in generic power conditioners designed to function with a variety of array types, sizes and site locations.

In selecting various design parameters such as voltage-tracking strategy and current and voltage limits it should be kept in mind that a 1% loss in available energy is comparable to a 1% increase in total system cost. For a present day (1982) system costing $25/watt this implies that a cost increase of approximately $0.25 per watt can be justified to achieve a 1% performance improvement.

PRECEDING PAGE BLANK NOT FILMED

PAGE 48 INTENTIONALLY BLANK

SECTION VIII

REFERENCES

1. Ross, R.G., Jr., and Gonzalez, C.C., "Reference Conditions for Reporting Terrestrial Photovoltaic Performance," Proceedings of the 1980 Annual Meeting of AS/ISES, Phoenix, Arizona, pp. 1091-1097.

2. Wen, L., An Investigation of the Effect of Wind Cooling on Photovoltaic Arrays, JPL Publication 82-28, JPL Document No. 5101-201, DOE/JPL-1012-69, Jet Propulsion Laboratory, Pasadena, California, March 1982.

3. Climates of the States, Volumes 1 and 2, National Oceanic and Atmospheric Administration, U.S. Dept. of Commerce, Water Information Center, Inc., Port Washington, New York, 1974.

4. Smith, J.H., Handbook of Solar Energy Data for South-Facing Surfaces in the United States, Volumes II and III, JPL Publication 79-103, JPL Document No. 5101-91, DOE/JPL-1012-25, Jet Propulsion Laboratory, Pasadena, California, January 1980.

PRECEDING PAGE BLANK NOT FILMED

PAGE 50 INTENTIONALLY BLANK